Observatório Nacional

Divisão de Programas de Pós-Graduação

MODELAGEM TERMOMECÂNICA E CINEMÁTICA DAS BACIAS INTRACONTINENTAIS DO TIPO RIFTE DA REGIÃO DO VALE DO CARIRI, PROVÍNCIA BORBOREMA, NE DO BRASIL

Pedro Correia Pessano

Dissertação apresentada ao Programa de Pós-graduação em Geofísica do Observatório Nacional, como parte dos requisitos necessários à obtenção do título de Mestre em Geofísica.

Orientador(a): Dr. Leandro Di Bartolo

Co-orientadores: Dr. Carlos Eduardo Ganade de Araujo
Dr. Victor Sacek

Rio de Janeiro
Junho de 2023

MODELAGEM TERMOMECÂNICA E CINEMÁTICA DAS BACIAS INTRACONTINENTAIS DO TIPO RIFTE DA REGIÃO DO VALE DO CARIRI, PROVÍNCIA BORBOREMA, NE DO BRASIL

Pedro Correia Pessano

DISSERTAÇÃO SUBMETIDA AO PROGRAMA DE PÓS-GRADUAÇÃO EM GEOFÍSICA DO OBSERVATÓRIO NACIONAL COMO PARTE DOS REQUISITOS NECESSÁRIOS PARA A OBTENÇÃO DO TÍTULO DE MESTRE EM GEOFÍSICA.

Examinada por:

Dr. Leandro Di Bartolo

Dr. Renato Darros de Matos

Dr. Emanuele Francesco La Terra

RIO DE JANEIRO, RJ – BRASIL
JUNHO DE 2023

"MODELAGEM TERMOMECÂNICA E CINEMÁTICA DAS BACIAS INTRACONTINENTAIS DO TIPO RIFTE DA REGIÃO DO VALE DO CARIRI, PROVÍNCIA BORBOREMA, NE DO BRASIL"

Pedro Correia Pessano

DISSERTAÇÃO SUBMETIDA AO CORPO DOCENTE DO PROGRAMA DE PÓS-GRADUAÇÃO EM GEOFÍSICA DO OBSERVATÓRIO NACIONAL COMO PARTE DOS REQUISITOS NECESSÁRIOS PARA A OBTENÇÃO DO GRAU DE MESTRE EM GEOFÍSICA.

Aprovada por:

_____

Dr. Leandro Di Bartolo - (Orientador)-(ON)

_____

Dr. Emanuele Francesco La Terra - (ON)

_____

Dr. Renato Darros de Matos - (Pesquisador - Consultor independente)

RIO DE JANEIRO – BRASIL

28 DE FEVEREIRO DE 2023

Lista de signatários

5/5 Assinaturas efetuadas

PEDRO CORREIA PESSANO E-mails enviados

Assinou

Verificação do nome: Nome confere com a base de dados da Receita Federal.

Data da assinatura: 2 de março de 2023 às 14:48

Ver mais

LEANDRO DI BARTOLO E-mails enviados

Assinou

Verificação do nome: Nome confere com a base de dados da Receita Federal.

Data da assinatura: 3 de março de 2023 às 12:33

Ver mais

EMANUELE FRANCESCO LA TERRA E-mails enviados

Assinou

Verificação do nome: Nome confere com a base de dados da Receita Federal.

Data da assinatura: 5 de março de 2023 às 20:01

Ver mais

RENATO MARCOS DARROS DE MATOS E-mails enviados

Assinou

Verificação do nome: Nome confere com a base de dados da Receita Federal.

Data da assinatura: 16 de março de 2023 às 14:46

Ver mais

GIANE DO CARMO BOLDRIM E-mails enviados

Assinou

Verificação do nome: Nome confere com a base de dados da Receita Federal.

Data da assinatura: 17 de março de 2023 às 13:12

Correia Pessano, Pedro

Modelagem termomecânica e cinemática das bacias intracontinentais do tipo rifte da região do Vale do Cariri, Província Borborema, NE do Brasil/Pedro Correia Pessano. – Rio de Janeiro: ON, 2023.

??, 48 p. 29, 7cm.

Orientador(a): Leandro Di Bartolo

Co-orientadores: Carlos Eduardo Ganade de Araujo

Victor Sacek

Dissertação (mestrado) – ON/Programa de Pós-graduação em Geofísica, 2023.

Referências Bibliográficas: p. 40 – 48.

1. Thermomechanical modeling. 2. Numerical scenarios. 3. Proterozoic inheritances. 4. Rift nucleation. 5. Borborema Province. I. Ganade de Araujo, Carlos Eduardo *et al.* II. Observatório Nacional, Programa de Pós-graduação em Geofísica. III. Título.

Agradecimentos

Agradeço primeiramente a Deus, que me deu forças e me conduziu por todo o caminho. Sem Ele, nada disso teria sido possível. Também não teriamos as maravilhas da natureza para serem estudadas.

Aos meus pais, Carmen e Jorge Pessano, por todo o amor e apoio, e pelo demasiado investimento na minha formação pessoal e profissional.

À minha irmã, Helena, pelos nossos bons momentos na infância e pela pessoa inspiradora que ela se tornou.

À Giovana, minha futura esposa e melhor amiga, por sempre me inspirar, me incentivar a dar o meu melhor, apoiar as minhas ideias e pelos maravilhosos momentos juntos.

Ao meu orientador, Leandro Di Bartolo, por ter aceitado ser o meu tutor, e por ter ensinado um geólogo os primeiros passos de computação e modelagem.

Aos meus coorientadores, Carlos Eduardo Ganade (Caê) e Victor Sacek, por confiado em mim para realizar um projeto fora da minha área de expertise.

À Rafael Monteiro da Silva, aluno de pós-Doutorado da USP, que muito me ajudou na implementação dos modelos numéricos.

Ao pessoal do LabSisCon do Observatório Nacional, que me ajudaram à colocar as simulações para rodar no workstation.

Ao Observatório Nacional e seu excelente corpo docente, que me receberam de braços abertos e que muito me ensinaram.

E a todos aqueles que, de alguma forma ou outra, estiveram presentes nessa jornada. Muito obrigado!

Resumo da Dissertação apresentada ao Programa de Pós-Graduação em Geofísica do Observatório Nacional como parte dos requisitos necessários para a obtenção do título de Mestre em Geofísica.

MODELAGEM TERMOMECÂNICA E CINEMÁTICA DAS BACIAS INTRACONTINENTAIS DO TIPO RIFTE DA REGIÃO DO VALE DO CARIRI, PROVÍNCIA BORBOREMA, NE DO BRASIL

Pedro Correia Pessano

Junho/2023

O papel das heranças Proterozoicas na Província da Borborema, nordeste do Brasil, na formação e evolução das bacias rift do Cretáceo Inferior é amplamente aceito pela comunidade científica, mas algumas causas subjacentes ainda são incertas. Nesse caso, as zonas de cisalhamento continentais têm sido amplamente atribuídas como sendo as heranças mais relevantes, com alguns estudos mostrando que novas falhas se originaram a partir delas durante o estiramento litosférico. Neste trabalho, utilizamos modelagem numérica geodinâmica para investigar o rifteamento e a formação de bacias no Vale do Cariri, a fim de avaliar o papel das heranças Proterozoicas nesse processo. Os cenários numéricos demonstram que a configuração reológica é a característica mais proeminente, principalmente o acoplamento entre a crosta superior e o manto litosférico, bem como a heterogeneidade lateral do manto. A localização do rifte ocorre em camadas fracas dentro da litosfera, e as heterogeneidades mantélicas desempenham um papel importante na localização da deformação em comparação com as heterogeneidades crustais. As zonas de cisalhamento foram reativadas de forma frágil apenas após o início do rifteamento e ajudaram a delimitar a largura das bacias.

Abstract of the Dissertation presented to the National Observatory's Graduate Program in Geophysics as a partial fulfillment of the requirements for the degree of Master in Geophysics.

THERMOMECHANICAL AND KINEMATIC MODELING OF INTRACONTINENTAL RIFT BASINS IN THE CARIRI VALLEY REGION, BORBOREMA PROVINCE, NE BRAZIL

Pedro Correia Pessano

June/2023

The role of the Proterozoic inheritances of the Borborema Province, NE Brazil, on the formation and evolution of Early Cretaceous rift basins is highly accepted by the scientific community, but some underlying causes are still uncertain. The continental shear zones have been widely assigned as being the most relevant inheritances in this case, with some works showing that new faults nucleated from them during the lithospheric stretching. In this work, we use geodynamic numerical modeling to investigate rifting and basin-formation in the Cariri Valley, such as to assess the role of Proterozoic inheritances in the process. The numerical scenarios demonstrate that the rheological configuration is the most prominent feature, mainly the coupling between the upper crust and the lithospheric mantle, as well as the lateral heterogeneity of the mantle. Rifting location occurs in weak layers within the lithosphere, and mantelic heterogeneities have a major role in strain localization when compared to crustal heterogeneities. The shear zones were brittle reactivated only after the onset of rifting and helped to delimit the width of the basins.

Contents

List of Figures

List of Tables

Chapter 1

Introduction

Rifting is one of the most important geological phenomena in tectonics, and geodynamics, as it represents an essential mechanism for the formation of sedimentary basins, and the evolution of the lithosphere. Rift basins cover large areas of the globe and contain relevant mineral deposits and energy resources (CLOETINGH *et al.*, 2015). Understanding their formation and the process behind it is a matter of great importance not only for the academy but also for industry, especially Oil & Gas.

The Cariri Valley belongs to the Northeast Brazilian Rift System (MATOS, 1992), which corresponds to a set of rift basins in the easternmost tip of South America that is associated with the intersection of the Southern and Equatorial branches of the South Atlantic Cretaceous Rift System (MATOS, 2000, 1999, 1992; MATOS *et al.*, 2021). The formation of this system has been dated as Lower Cretaceous (SZATMARI *et al.*, 1987), although, in order to understand its formation, it is necessary to look back to the Precambrian geology of the Borborema Province.

According to MATOS *et al.* (2021) and MATOS (1999), the Brasiliano shear zones of the Borborema Province played a fundamental role in the evolution of the South Atlantic rifts. The Proterozoic inheritance of the Borborema behaved as a "lithospheric relay ramp" and acted as the main obstacle to the opening of the South Atlantic (MATOS *et al.*, 2021).

The vast literature on the influence of inherited structures in controlling lithospheric dynamics (e.g., MATOS, 1999, 1992; MATOS *et al.*, 2021; VIOLA *et al.*, 2005, 2012; WILL & FRIMMEL, 2018) rely most on field observations, laboratory analysis, data compilation, and correlation, which is not an issue. However, as geodynamic processes occur in long (and varying) intervals, the dynamic description of such phenomena is a powerful tool that shows the evolution of the system through time (STÜWE, 2007).

The absence of numerical modeling works in the Cariri Valley rift basins hinders the discovery of the underlying causes behind their evolution. The literature al-

ready states that the Proterozoic inheritance was fundamental in the rifting process (MATOS *et al.*, 2021), nevertheless, the thermomechanical and kinematic behavior of the lithosphere during the extension is still unclear. Numerical models allow us to test different initial boundary conditions, rheological and physical parameters, and watch their response to deformation over time (STÜWE, 2007).

Therefore, the geodynamic numerical modeling of the Cariri Valley rift basins is a novel approach in the study of the northeastern intracontinental basins of Brazil and provides new data on lithospheric physics, and the rheological effects of Proterozoic structures in the tectonics.

Chapter 2

Geological settings and tectonics

2.1 Borborema's Precambrian geology

The Borborema Province (BP), northeastern Brazil, consists of a complex mosaic of Archean to Paleoproterozoic gneiss-migmatite complexes and metasedimentary belts that amalgamated during the West Gondwana Orogeny (or Brasiliano Orogeny) from 620 to 570 Ma, covered by remnants of Paleozoic and Mesozoic sedimentary basins (Fig. 2.1) (ALMEIDA *et al.*, 1981; ARTHAUD *et al.*, 2008; BRITO NEVES *et al.*, 2000; GANADE *et al.*, 2014; NEVES, 2003; OLIVEIRA & MEDEIROS, 2018). It covers an area of about 400,000 km^2 and is delimited by the São Francisco Craton (SFC) to the south, the Parnaíba Basin to the west, and the Atlantic continental margin to the north and east (Fig. 2.1) (ALMEIDA *et al.*, 1981; BRITO NEVES *et al.*, 2000; CABY *et al.*, 1991).

The region is subdivided by the E-W trending Patos and Pernambuco shear zones into three major tectonic domains: Southern, Central (or Transversal), and Northern, which is further subdivided into the Rio Grande do Norte, Ceará Central, and Médio-Coreaú domains (ARTHAUD *et al.*, 2008; BRITO NEVES *et al.*, 2000; GANADE *et al.*, 2014; NEVES, 2003). These domains are characterized by a pronounced lithological heterogeneity, a series of conjugate shear zones, and Neoproterozoic plutonism (Fig. 2.1) (ARTHAUD *et al.*, 2008; BRITO NEVES *et al.*, 2000; GANADE *et al.*, 2014; MATOS, 1999; NEVES, 2003).

Many works report the complex lithology of the BP (e.g., ALMEIDA *et al.*, 1981; ARTHAUD *et al.*, 2008; BRITO NEVES *et al.*, 2000, 2014; CABY *et al.*, 1991). Archean rocks were identified in the São José do Campestre block, northeastern corner of the Province, and comprise medium- to high-grade orthogneisses which yielded U-Pb zircon ages (SHRIMP) of 3400 Ma (DANTAS *et al.*, 2013). The Proterozoic sequences correspond to metasedimentary rocks derived from pre-Brasiliano sediments (CABY *et al.*, 1991). These rocks include paragneisses, schists,

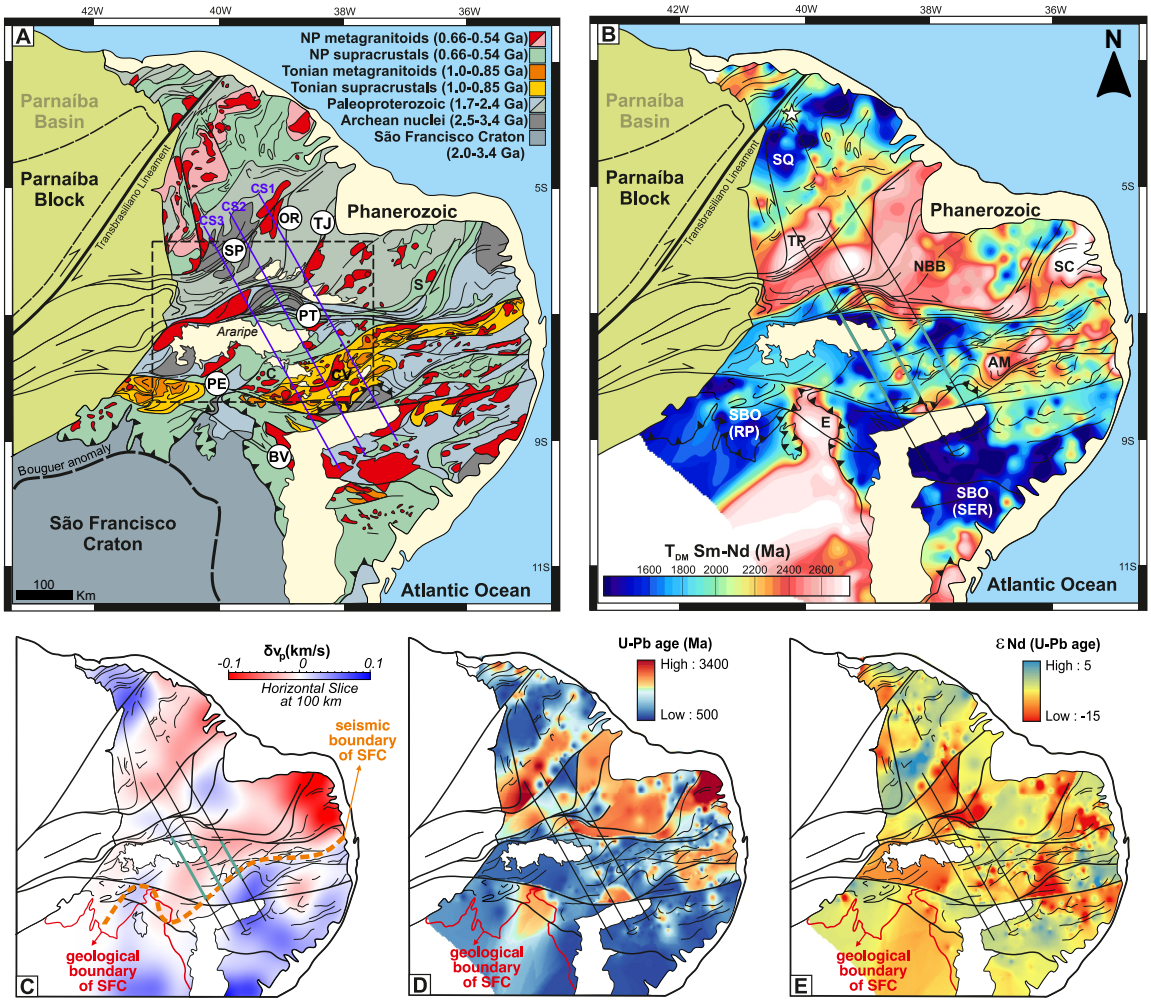

Figure 2.1: Mosaic of the Borborema Province geological features. A) Present-day geological map of the Borborema Province illustrating its complex lithological mosaic. Circle labels correspond to major shear zones. The dashed black rectangle refers to the area known as Cariri Valley. Purple thick lines indicate the cross-sections 1, 2, and 3 (CS1, CS2, and CS3; Fig. 2.2). C, S, and CV correspond, respectively, to the Cachoeirinha and Seridó belts, and the Cariris-Velhos terrane. BV: Boa Vista shear zone, OR: Orós shear zone, PT: Patos shear zone, PE: Pernambuco shear zone, SP: Senador Pompeu shear zone, TJ: Tatajuba-Jaguaribe shear zone. Geological base maps are from the Geological Survey of Brazil available at http://geosbg.cprm.gov.br. B) Sm-Nd T_{DM} age map of the Borborema Province and northern São Francisco Craton with the magnetic first derivative image as the background. The greenish thick lines indicate the width of the modified mantle beneath. AM: Alto Motoxó terrane, E: Entremontes block, NBB: Northern Borborema block, RP: Riacho do Pontal fold-and-thrust and belt, SQ: Santa Quitéria block, SC: São José do Campestre terrane, SER: Sergipano fold-and-thrust belt, SBO: Southern Borborema block, TP: Tróia-Pedra Branca terrane. C) P-wave tomography model for the BP at 100 km depth. D) Spatial distribution of of zircon U-Pb crystallization ages of igneous and metaigneous rocks of the Borborema Province. E) Spatial distribution of $\epsilon_{Nd(t)}$ values calculated for U-Pb ages shown in D. The grids exhibited in C, D, and E were built in ArcGis using the Inverse-Distance-Weighted Interpolation. Adapted from GANADE *et al.* (2021).

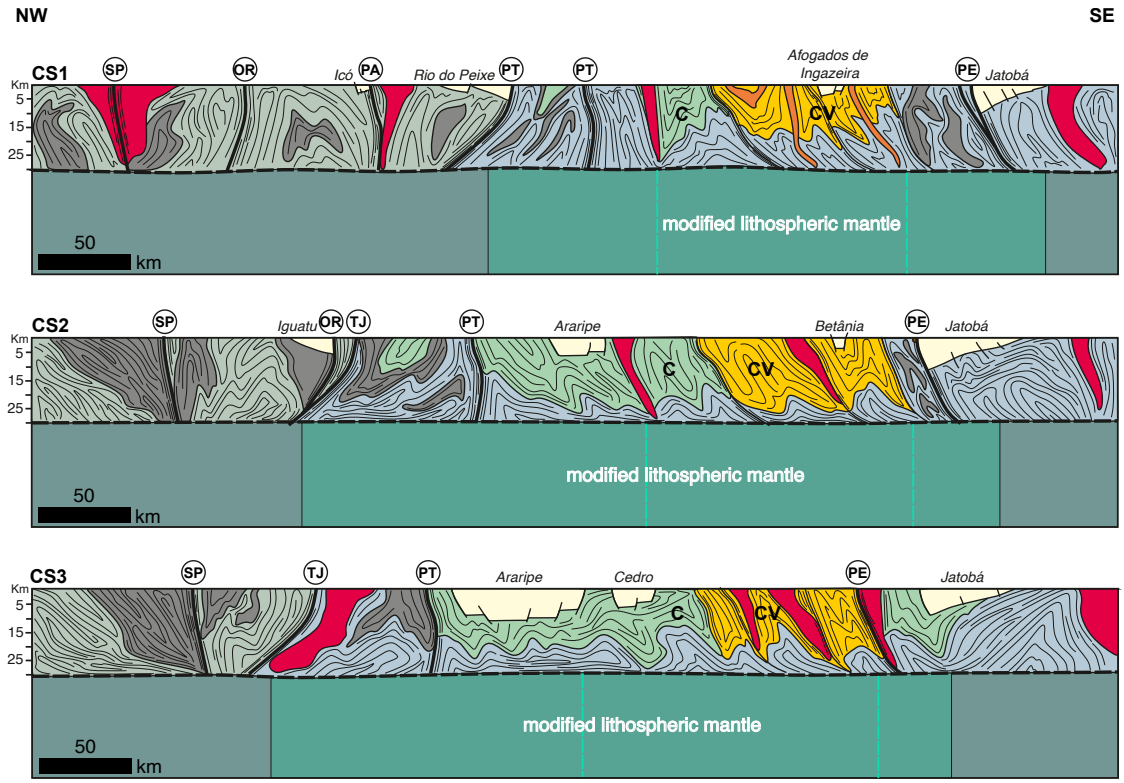

Figure 2.2: Geological cross-sections showing the lithological variety of the Borborema Province and its main features. The upper portion of the lithospheric mantle is also shown, but with no detail. The color legend is the same adopted in figure 2.1. Turquoise dashed lines in the lithospheric mantle refer to the alternate width of this layer used in some scenarios (see the results section). Circle labels correspond to major shear zones. C, S, and CV correspond, respectively, to the Cachoeirinha and Seridó belts, and the Cariris-Velhos terrane. OR: Orós shear zone, PA: Portalegre shear zone, PT: Patos shear zone, PE: Pernambuco shear zone, SP: Senador Pompeu shear zone, TJ: Tatajuba-Jaguaribe shear zone. Based on GANADE *et al.* (2021).

carbonate lenses, and quartzites (BRITO NEVES *et al.*, 2000, 2014; CABY *et al.*, 1991; NEVES, 2003, and references therein). In addition to the metamorphism, deformation, and shearing, the Brasiliano orogeny produced several types of granitoid that are seen throughout the Province (Fig. 2.1) (ARTHAUD *et al.*, 2008; CABY *et al.*, 1991; GANADE *et al.*, 2014; NEVES, 2003, and references therein).

According to VAUCHEZ *et al.* (1995), the shear zones are usually mylonitic, but also present migmatites, syn- to late-kinematic plutons, and dikes in their composition. Their widths range from 1 km for the subsidiary faults, up to 10 km for the Pernambuco and Senador Pompeu shear zones, and 25 km for the Patos SZ (VAUCHEZ *et al.*, 1995).

2.2 The Northeast Brazilian Rift System

The Northeast Brazilian Rift System is located in the easternmost tip of South America and corresponds to an extensive complex of rift basins formed on the Borborema Province during the opening of the South Atlantic Ocean in the Lower Cretaceous (MATOS, 1992). In this work, we focus on the Cariri-Valley, a set of aborted rift basins in the heart of the Borborema Province (Fig. 2.3).

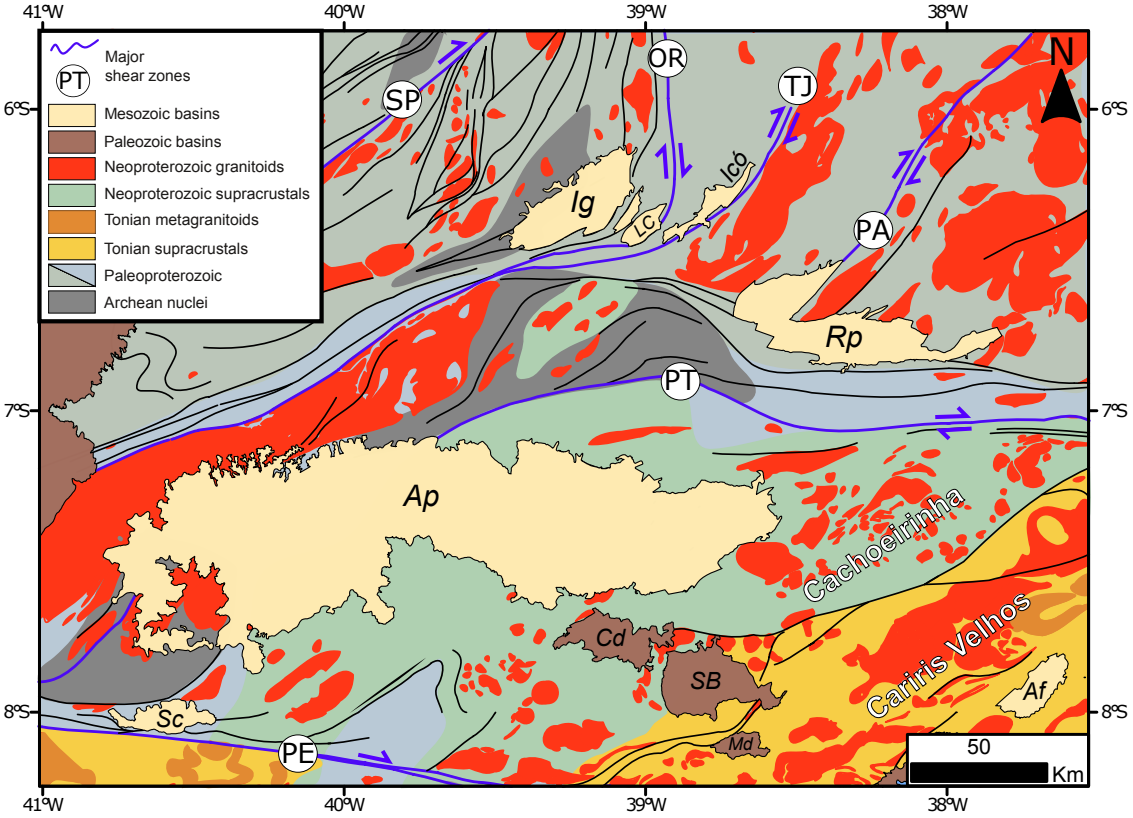

Figure 2.3: Structural framework and distribution of the main syn-rift basins (Rift Stage II) of the Cariri Valley. It is seen that the E-W direction of the Araripe Basin is generally controlled by the Patos Shear Zone and the conjugate sets that branch out of it. Major shear zones are represented by thick purple lines. Af: Afogados de Ingazeira basin, Ap: Araripe basin, Cd: Cedro basin, Ig: Iguatu basin, LC: Lima Campos basin, Md: Mirandiba basin, Rp: Rio do Peixe, SB: São José de Belmonte basin, Sc: Socorro Santo-Inácio basin. Geological base maps are from the Geological Survey of Brazil available at http://geosbg.cprm.gov.br. Adapted from MATOS (1999).

The complex framework of Borborema Province (Borborema-Benin Nigerian Province at the time) played a relevant role in the coupled opening of the Equatorial South Atlantic and the formation of intracontinental rift basins (MATOS, 2000, 1999, 1992; MATOS *et al.*, 2021). According to MATOS (1999, 1992) and MATOS *et al.* (2021), the Proterozoic inheritance controlled the pattern of opening and linkage of the rift zones (Fig. 2.4). WILL & FRIMMEL (2018). Based on data from the South Atlantic Margins, rifting usually occurs in rheologically weakened

domains and is related to far-field forces. This corroborates the studies of VIOLA *et al.* (2005, 2012), who argued that present-day seismicity and neotectonic in SW Africa is controlled by the Pan-African inheritance.

Previous studies (e.g., MATOS, 2000, 1999, 1992; MOHRIAK *et al.*, 2000) recognized that three tectonic stages, Syn-rift I, II, and III, marked the stepwise opening of the South Atlantic. They are distributed over three main rift axes: 1) Gabon-Sergipe-Alagoas; 2) Recôncavo-Tucano-Jatobá; 3) Cariri-Potiguar, and each one features a different main extension direction (MATOS, 1999, 1992). Recently, MATOS *et al.* (2021) divided the rifting process into six rift stages. Each stage mark a regional event that caused a significant impact on the tectono-stratigraphic environment of a certain portion of the margin, they do not refer to chronostratigraphic boundaries (MATOS *et al.*, 2021).

The following description of the rift stages can be seen in detail in the original work of MATOS *et al.* (2021) and references therein. The Rift Stage I (145-140 Ma) is identified by the onset of the oldest rift axes of Demerara-Marajó, West and Central African, and Recôncavo-Tucano-Jatobá/Gabon-Sergipe-Alagoas. They were triggered solely by the distribution and partitioning of intracontinental strain with minor magmatic activity. Rift Stage II (140-126 Ma) exhibits more interaction between plate dynamics, rifting, and magmatism. During this phase, South America was rotating clockwise about a pole in northern Brazil, and two Large Igneous Provinces (LIPs) were taking place, Paraná-Etendeka (southern Brazil) and Borborema (northeastern Brazil), also named as Equatorial Atlantic Magmatic Province (EQUAMP) in HOLLANDA *et al.* (2018) and PESSANO *et al.* (2021). Also, the opening of the Cariri-Potiguar-West Africa axes started during this period.

The third stage (126-123 Ma) encompasses the continuation of the clockwise rotation with dextral strike-slip faulting in the equatorial margin and the incipient delineation of the South American and African borders. For the purpose of this work, two events that occurred in this phase must be highlighted: the abortion of the Cariri-Potiguar and Recôncavo-Tucano-Jatobá axes and their post-rift sedimentation (Fig. 2.3), and the confirmation of the Borborema-Benin Nigerian Province as a continental-scale relay zone that mechanically balanced the rift propagation of the South and Central Atlantic.

Rift Stage IVa (123-117 Ma) is marked by simultaneous rifting along the South Atlantic margin, the definition of the South American and African lithospheric boundaries, and, most important, the formation of the pre-salt deposits. The Rift stage IVb (117-113 Ma) is characterized by the restricted marine environment which allowed the formation of a massive salt deposit (Aptian Salt Age). At last, the Rift Stage V (113-100.5 Ma) is when the South Atlantic breakup reaches its climax with seafloor spreading between South America and Africa, formation of proto-transform

faults at the Equatorial Atlantic, and a late marine magmatic pulse related to the Borborema (or EQUAMP) LIP (MATOS *et al.*, 2021, and references therein).

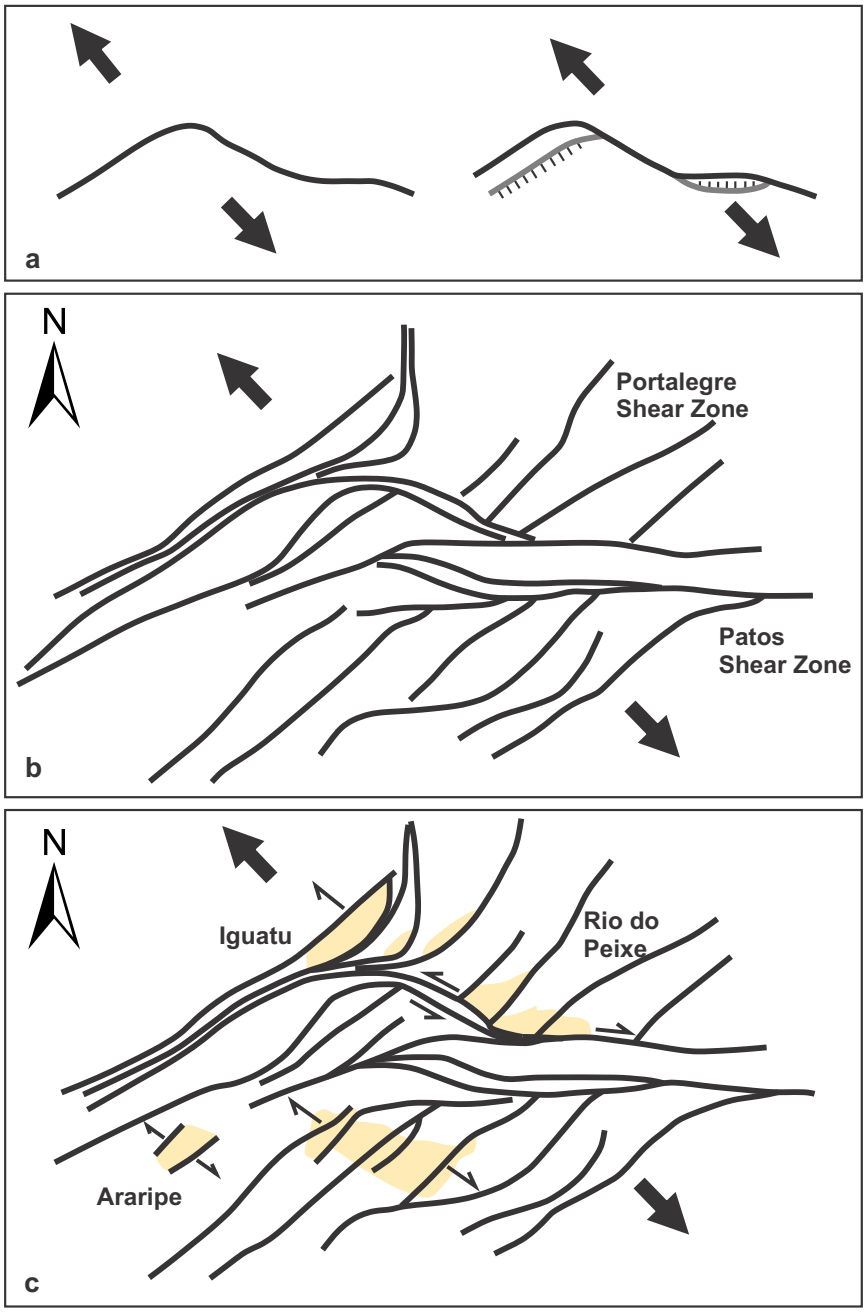

Figure 2.4: Schematic model of the tectonic evolution of the Cariri Valley intracontinental rift basins. This figure illustrates the influence of the Proterozoic inheritance in the formation of the rift basins of the Cariri Valley. a, b) NW-SE extension during Rift Stage II reactivated most of the sigmoidal-shaped Brasiliano shear zones; c) NE-SW trending asymetric half-grabens separated by basement highs, transfer faults and/or accommodation zones. Extracted from MATOS (1999).

Chapter 3

The Proterozoic inheritances

The definition of 'inheritance' and its role in rifting is a deeply discussed topic in tectonics and geodynamics. Here, based on the works of MANATSCHAL *et al.* (2015) and MANATSCHAL *et al.* (2021), we consider 'inheritance' as the innate characteristic of a terrain, a 'geological genetic code'. It is not only an inborn feature, it is mainly the product of numerous tectonic, magmatic, and metamorphic events that occur in the region over time (MANATSCHAL *et al.*, 2015, 2021).

Rifting in continental domains is highly influenced by inheritances (MANATSCHAL *et al.*, 2015, 2021; VIOLA *et al.*, 2005, 2012; WILL & FRIMMEL, 2018). The general agreement is that the complex lithological and structural record of the continents hinders the interpretation of their original state at the onset of rifting (MANATSCHAL *et al.*, 2015, 2021).

In this paper, we distinguish between two inheritance types for the Borborema Province, namely structural and compositional. The structural inheritances refer to the shear zones and their influence, while the compositional inheritances correspond to the lithological controls on the rifting process (e.g., MANATSCHAL *et al.*, 2015).

3.1 Structural inheritances

Structural inheritances can be understood as mechanically weak zones that resulted from previous orogenic events that deformed the lithosphere (MANATSCHAL *et al.*, 2015). SCHIFFER *et al.* (2020) defines structural inheritance as a geological property, especially of the continental lithosphere, that guides deformation along preexisting rheological heterogeneities at all scales. In this case, as mentioned before, the shear zones of the Borborema Province are the structural inheritances in question. Such zones correspond to strong heterogeneities and are usually the product of an orogenic event in a ductile layer (MANATSCHAL *et al.*, 2015; TOMMASI & VAUCHEZ, 2001).

TOMMASI & VAUCHEZ (2001) suggest that these inheritances may induce strain localization and guide the propagation of the initial instability. During the opening of the Atlantic Ocean, the shear zones accommodated the extensional strain (MATOS, 1999; MATOS *et al.*, 2021) and their reactivation, apparently, allowed the nucleation of normal faults (MATOS, 1999; MATOS *et al.*, 2021; RAMOS *et al.*, 2022) (Fig. 2.4). Moreover, they also prevented and postponed the link between neighboring rift branches (MATOS, 1999; MATOS *et al.*, 2021).

The paragraph above can be explained by two important characteristics of the shear zones: i) their subvertical foliation - and its associated mineral-stretching lineation - may work like the lattice preferred orientation (LPO) of TOMMASI & VAUCHEZ (2001), and thus would be the main element controlling strain localization; ii) the rigid mylonitic composition (VAUCHEZ *et al.*, 1995) developed strong rheology that prevented the shear zones from breaking apart during rifting and the connection of rift branches (MATOS *et al.*, 2021). Although shear zones are relevant features in the rifting processes and are closely related to the The Northeast Brazilian Rift System, the work of RAMOS *et al.* (2022) show that their mylonitic foliation did not work as the weakness responsible for the brittle reactivation

Although inherited structures play a relevant role in rifting, not every inheritance has the potential to be reactivated or affect rifting by itself (CHENIN & BEAUMONT, 2013; MANATSCHAL *et al.*, 2015). The stretching direction relative to the structure (e.g., oblique, parallel, normal), the magnitude and lateral continuity, and the rheological contrast of the surrounding rocks, including other lithospheric layers, are also important factors to be taken into account (e.g, CHENIN & BEAUMONT, 2013; MANATSCHAL *et al.*, 2015; RING, 1994; TOMMASI & VAUCHEZ, 2001).

According to MUÑOZ-BARRERA *et al.* (2020), when reactivated, preexisting structures can: i) control the nucleation and localization of new faults, ii) cause perturbations in the stress field, iii) control the segmentation of faults and rift basins, iv) influence the length, orientation, spacing, and evolution of faults, and v) control the shape and evolution of necking zones. SAMSU *et al.* (2020) declares that these inheritances significantly control the orientation and distribution of faults and fractures of rift basins and the sediments within, still, the generation of new structures parallel to preexisting ones does not always occur.

3.2 Compositional inheritances

Compositional inheritance, as defined by MANATSCHAL *et al.* (2015), is the difference between the real lithosphere, a heterogeneous mixture of rocks, and the idealized "layer cake" lithosphere, an overlapping set of layers with homogenous rheology. Figure 2.2 exhibits the complex compositional (and structural) heterogeneity

of the Borborema Province.

Basically, two kinds of terrains controlled the rifting of the Borborema Province, rigid gneiss migmatite terrains/granulite massifs, and weak metasedimentary/volcanic fold belts (MATOS, 1999; MATOS *et al.*, 2021). In the case of volcanic fold belts, GANADE *et al.* (2021) delve deep into the Cachoeirinha-Seridó belt and the Cariris-Velhos terrane (in this work, we will use the terms "Proterozoic", "Tonian Terranes", or even "fragile terranes" to refer to these old orogens). According to GANADE *et al.* (2021), both terranes passed through a process of decratonization due to continental rifting between 1.0-0.92 and 0.9-0.82 Ga, making them weaker than the surrounding rocks.

Furthermore, in contrast to the weak rheology of the Toninan terranes, GANADE *et al.* (2021) indicates that numerous processes of melting might have depleted their underlying lithospheric mantle, making it more rigid than the non-depleted mantle that occurs in the surrounding areas. Not only did the lithospheric mantle become stiffer with the extension of the cratonic lithosphere, but mafic magmatism at the base of the crust may have strengthened the lower crust and its coupling with the lithospheric mantle (GANADE *et al.*, 2021). Forward modeling of the bulk V_p/V_s ratio points to a little mafic underplate beneath the Borborema Platau (LUZ *et al.*, 2015), which corroborates with a higher degree of coupling between the mantle and the upper crust of the Tonian Terranes.

Nonetheless, another composition of the underlying lithospheric mantle can be assumed based on the work of CHENIN *et al.* (2019). They highlight that the mantle beneath embryonic oceans, such as the incipient and confined Sergipano Ocean (ca. 920 - 820 Ma; GANADE *et al.* 2021), is more fertile than other types of mantle, less dense, and mechanically weaker. Orogens that result from the closure of this type of ocean (e.g., Cariris Velhos Orogeny, 1.0-0.92 Ga) preserve the fertilized mantle beneath them. The inversion of a narrow oceanic basin exhibits minimal subduction and thus, is absent of depletion due to subduction-related magmatism (CHENIN *et al.*, 2019).

Chapter 4

Methodology

To simulate the geodynamic evolution of the crust and mantle through the geological time scale, we used the Mantle Dynamics Simulator Code (Mandyoc) (SACEK *et al.*, 2022; SILVA & SACEK, 2022). Mandyoc is a 2D finite element code that simulates thermomechanical convection in terrestrial planets and surface processes (SACEK *et al.*, 2022). Works on the evolution of the continental margin (e.g., SACEK, 2017; SALAZAR-MORA & SACEK, 2021; SILVA & SACEK, 2022) attest to the power and capabilities of the software. For more information and code examples, please see SACEK *et al.* (2022) and access Mandyoc's repository on GitHub. The software version used in the present work is v0.1.6.

4.1 Mandyoc's mathematics

In this numerical approach, the non-Newtonian fluids formulation was adopted with the extended Boussinesq approximation (ZHONG *et al.*, 2007), solving the following equations of conservation of mass, momentum, and energy, respectively

$$u_{i,i} = 0 \tag{4.1}$$

$$\sigma_{ij,j} + g\rho_0\alpha T\delta_{i3} = 0 \tag{4.2}$$

$$\frac{\partial T}{\partial t} + u_i T_{,i} = \kappa T_{,ii} + \rho_0 H - \alpha T g u_3/c_p \tag{4.3}$$

where

$$\sigma_{ij} = -P\delta_{ij} + \eta(u_{i,j} + u_{j,i}) \tag{4.4}$$

and t is time, u_i is the i-th component of the velocity field, g is the gravity acceleration, ρ_0 is the reference density, α is the volumetric coefficient of thermal expansion, T is temperature, κ is the thermal diffusivity, H is the radiogenic heat production per unit mass, P is the dynamic pressure, c_p is the specific heat capacity, η is the

effective viscosity of the rock and δ_{ij} is the Kronecker's delta. In this notation, repeated indexes represent sum and $T_{,i}$ is the partial derivative of T relative to the x_i coordinate.

In equation 4.3, the three terms in the right-hand side are, respectively, the component of thermal diffusion, heat production due to radiogenic heat, and adiabatic heating.

The different lithological layers are simulated by the visco-plastic rheology, where the effective viscosity η depends on a non-linear power law viscous component and a plastic yield criterion.

The plastic yield limit follows the Drucker–Prager criterion:

$$\tau_{yield} = c_0 \cos\phi + P \sin\phi \tag{4.5}$$

where c_0 is the internal cohesion and ϕ is the internal angle of friction.

The non-linear viscosity η_{visc} of the viscous rheology follows a power law function dependent on temperature, composition, and strain rate (HUISMANS & BEAUMONT, 2014):

$$\eta_{visc} = CA^{-1/n}\dot{\varepsilon}_{II}^{\frac{1-n}{n}} \exp\left[\frac{E_a + VP}{nRT}\right] \tag{4.6}$$

where C is a scale factor, A is the pre-exponential scale factor, n is the power law exponent, $\dot{\varepsilon}_{II} = \left(\frac{1}{2}\dot{\varepsilon}'_{ij}\dot{\varepsilon}'_{ij}\right)^{1/2}$ is the square root of the second invariant of the strain rate tensor, E_a is the activation energy, V is the activation volume, and R is the universal gas constant.

The effective viscosity η, presented in equation 4.4, is calculated as the minimum between η_{plast} and η_{visc}:

$$\eta = \min(\eta_{plast}, \eta_{visc}) = \min\left(\frac{\tau_{yield}}{2\dot{\varepsilon}_{II}}, \eta_{visc}\right). \tag{4.7}$$

The equations 4.1-4.2 are numerically solved using the finite element method (ZHONG *et al.*, 2007) in a three-dimensional mesh using hexahedral elements Q_1P_0 or a two-dimensional mesh using quadrilateral elements Q_1P_0 (HUGHES, 2012). Additionally, the equation 4.3 is solved over the same finite element mesh following the implicit formulation presented by BRAUN (2003).

For the numerical simulation (Fig. 4.1), initially the user specifies the initial and boundary conditions for temperature T and velocity u, along with the reference density field ρ_0, radiogenic heat production H and other rheological parameters. In each time step, η_{visc} and η_{plast} are calculated based on equations 4.5 and 4.6, respectively. Then the effective viscosity is determined from equation 4.7. With the effective viscosity η and boundary conditions for u, the Uzawa's method (ZHONG

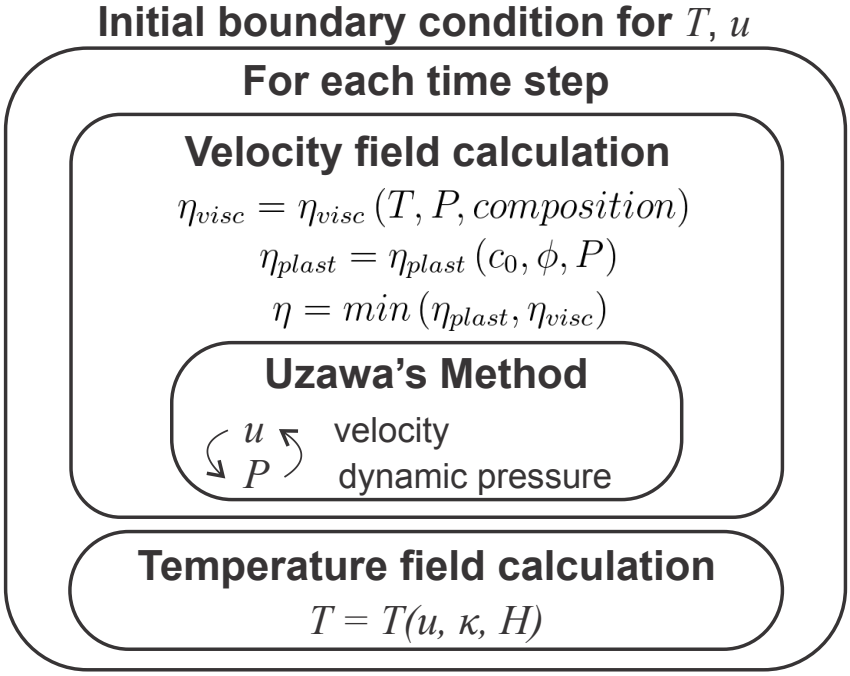

Figure 4.1: Flowchart for the numerical solution of the equations related to the conservation of mass, momentum, and energy.

et al., 2007) is applied to iteratively solve equations 4.1 and 4.2, obtaining a new field for u and P. The change in the velocity field modifies the effective viscosity η, changing the velocity field u again. These fields are updated until the following convergence criterion is achieved (THIEULOT, 2014):

$$\chi_f = 1 - \frac{\langle (f^i - \langle f^i \rangle) \cdot (f^{i+1} - \langle f^{i+1} \rangle) \rangle}{|f^i - \langle f^i \rangle| \; |f^{i+1} - \langle f^{i+1} \rangle|} \leq tol \tag{4.8}$$

where f represents the vector containing the values of the velocity components u for all the nodes of the mesh, *tol* is the tolerance parameter (adopted here a default value of 10^{-6} but adjustable by the user if necessary) and $\langle f \rangle$ is the mean value of f. The superscript i and $i+1$ represent two consecutive iterations in the same time step. With the velocity field u, the equation 4.3 is solved to obtain the new thermal field.

Additionally, material properties, like density, are updated through time following the advection equation:

$$\frac{\partial c_m}{\partial t} + u_i c_{m,i} = 0 \tag{4.9}$$

where c_m is any material property advected by the velocity field u. This equation is solved explicitly through particles randomly distributed in the interior of the mesh, mapped in the different finite elements. The displacement of these particles is a function of the velocity of the nodes adjacent to the particle (TACKLEY & KING,

2003), calculated through linear interpolation in each finite element.

The computational code was written in C and can be executed in parallel, using a modern tool for algebra operations in distributed memory environment: PETSc - *Portable, Extensible Toolkit for Scientific Computation* (BALAY *et al.*, 1997, 2019, 2020).

4.2 Model setup

The Earth and the geodynamic processes that occur inside it are inherently three-dimensional. Therefore, it is very logical to assume that a model that realistically simulates the dynamics of the planet should also be developed in three dimensions. However, although 3D modeling seems to be a more logical and natural approach, it is actually much more computationally expensive when compared to 2D models (GERYA, 2010).

In spite of its limitations, we used a two-dimensional layered cross section to study the importance of inheritances in the rifting process. The heterogeneous layered structure of the Earth (i.e, upper and lower crust, lithospheric mantle, and asthenosphere) plays a crucial role in the whole process, and it can be appraised in a two-dimensional model (e.g., GERYA, 2010; SILVA & SACEK, 2022).

In the following sections, we split the explanation of the model into two parts: the first focuses on the interfaces and boundary conditions, and the second on the rheological and parameters and initial strain of the layers.

4.2.1 Numerical setup and boundary conditions

Interfaces are numerical structures delimited by a pair of top and bottom coordinate arrays that seek to represent the geometries and dimensions of a geological object in the real world. Together, these structures make up the numerical model (Fig. 4.2). The scenarios are based on the geological cross-sections depicted in figure 2.2.

In general, the models consist of, from bottom to top: i) asthenosphere, ii) lithospheric mantle, iii) lower crust, iv) upper crust, v) Proterozoic fragile terranes, vi) shear zones, and vii) "sticky air" (Fig. 4.2). The latter is a 40 km-thick layer with the density of air (zero) and a viscosity million times greater than that of air (Table 4.1; GERYA, 2010; GERYA & YUEN, 2003). This fictional layer is applied to attenuate unwanted deformation in the upper layer (i.e., upper crust; GERYA, 2010; GERYA & YUEN, 2003), and to ensure a free slip condition. Particularities of each interface will be discussed later, if necessary.

The model has a domain of 520×300 km^2 and is composed of a regular mesh

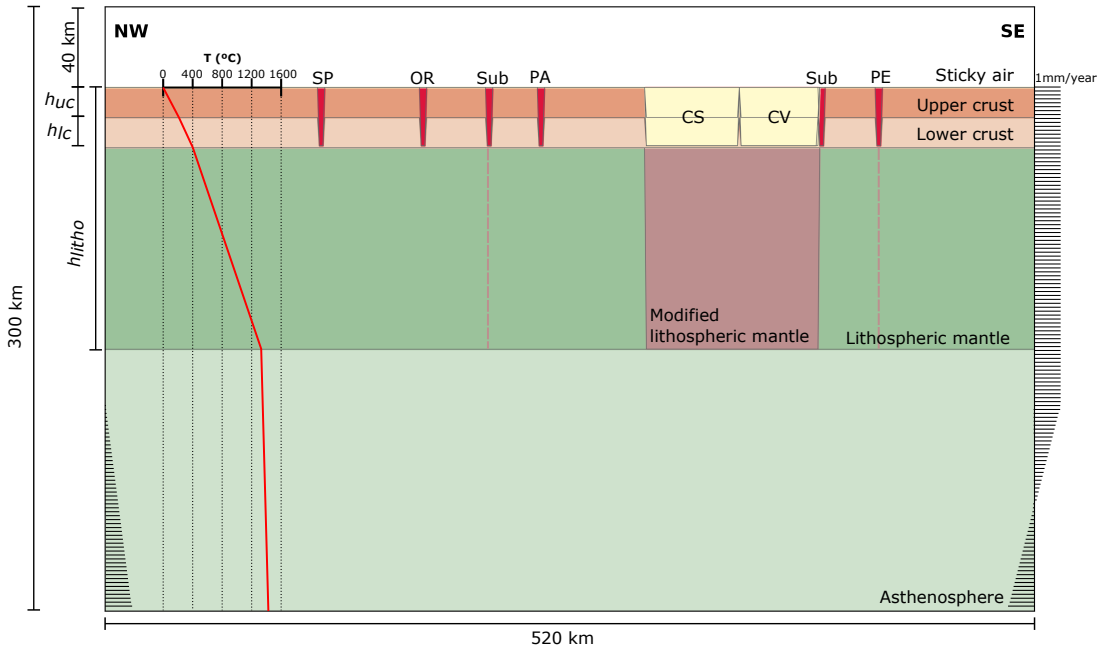

Figure 4.2: Numerical interfaces for the 2D cross section models depicted in this work. This scenario is based on the sections (CS1, CS2, and CS3) marked in fig. 2.1 and detailed in fig.2.2, but at 140 Ma, before the onset of rifting and the formation of the sedimentary basins. The thickness of the upper (h_{uc}) and lower crust (h_{lc}) are equal to 15 km, and the thickness of the lithosphere (h_{litho}) is 130 km. The velocity field is marked by a series of horizontal black lines on the sides of the model. The thermal profile is indicated in the graph and further detail can be seen in the text. For the reference model (see the results section), the 'Modified Lithospheric Mantle' in brown is not considered. Dashed brown lines refer to an alternate width of the modified mantle used in the "wide mantle" scenarios. SP: Senador-Pompeu Shear Zone; OR: Orós Shear Zone; Sub: Subsidiary shear zones; PA: Patos Shear Zone; PE: Pernambuco Shear Zone; CS: Cachoeirinha-Seridó belt; CV: Cariris Velhos terrane. This scenario is based on the work of SILVA & SACEK (2022), and Mandyoc's examples in SACEK *et al.* (2022) or at https://github.com/ggciag/mandyoc.

with square elements of 1x1 km^2. In order to simulate the lithospheric stretching, we used a reference frame fixed on the left 'plate' (i.e., the first half of the model), and a moving 'plate' on the right with a velocity of $1.6 - 2.0$ mm/year (Fig. 4.2; SILVA & SACEK, 2022). The adopted stretching rate is based on the work of HEINE *et al.* (2013) and data compiled by BONIFACIO *et al.* (2023). The conservation of mass, an essential characteristic of the numerical scenario, is achieved by a symmetrical velocity field (i.e., both sides of the model must have the same velocity, but in different directions).

The initial temperature profile was set to be only depth-dependent and defined as 0°C at the surface and 1300°C at the base of the lithosphere at 130 km (Fig. 4.2) (SILVA & SACEK, 2022). These boundary conditions are considered in the following equation, which solution gives the initial temperature structure of the interior of the lithosphere (SACEK *et al.*, 2022; SILVA & SACEK, 2022):

$$\kappa \frac{\delta^2 T(z)}{\delta z^2} + \frac{H(z)}{c_p} = 0 \tag{4.10}$$

where $H(z)$ is the internal heat production of the layer (Table 4.1). In the asthenosphere, the temperature model is defined by an adiabatic increase down to the bottom of the domain, as follows (SACEK *et al.*, 2022; SILVA & SACEK, 2022):

$$T = T_p \exp(\frac{g\alpha z}{c_p}) \tag{4.11}$$

where $T_p = 1262°C$ is the adopted potential temperature for the mantle (SILVA & SACEK, 2022). It is important to affirm that, during the simulations, the temperature in every boundary was maintained fixed. Figure 4.2 exhibits the temperature profile and how it changes across the layers.

The scenarios also have a denudation factor, which is simulated by the adoption of a bed erosion rate variable in space and time (e.g., SILVA & SACEK, 2022). The rate of erosion $\dot{e} = \dot{e}(x,t)$ is given by the following expression:

$$\dot{e} = \kappa_{sp} e_f(x) c_f(t) \tag{4.12}$$

where e_f is a spatial control on denudation, given by:

$$e_f(x) = \exp\left(-\frac{(x - x_c)^6}{x_\sigma^6}\right) \tag{4.13}$$

with x_{sigma} controlling the spatial extent of the denudation from the position x_c, while c_f is a climate function that re-scales the magnitude of the denudation rate through time. Table 4.2 indicates the values for the different fixed parameters of the simulation, such as the surface parameters. The denudation rate $\dot{e}$ is only activated if the topography h is above sea level h_{sl}. For regions below the sea level (-1000 m), there are no surface processes. At last, the scenarios were developed in a way that during the first 1 Myr no erosion occurs ($c_f = 0$), after that, we impose $c_f = 1$ to deal with the denudation.

4.2.2 Rheology and initial strain

Rheology is the physical property that characterizes the behavior of a material under stress, that is, the property which controls the deformation or flow of some material (BUROV, 2015; GERYA, 2010; MORAES, 2016). According to BUROV (2015), the elastic and plastic properties of the lithosphere determine, at small scales, the formation and evolution of major geologic structures such as rifts and basins. Although the strength of lithospheric plates depends on their structure and rheological properties (BUROV, 2015, and references therein), the Byerlee's law of

brittle failure (BYERLEE, 1978) establishes that brittle rock strength is above all a function of pressure-depth and is almost independent of rock type. Also, it was confirmed by several laboratory studies that most rock types have similar angles of internal friction (30-33°) and small dilatation angles (∼10°), which explains why even highly stratified volumes of brittle rocks often behave as a uniform media, even ignoring inherited structures (BYERLEE, 1978). On the other hand, ductile deformation strongly depends on rheological parameters and some specific criteria such as grain size, macro, and microstructures, temperature, strain rate, fluid content, etc (BUROV, 2015). In summary, ductile behavior depends, in a nonlinear manner, on strain rate and thus on the timescale of the event, while brittle behavior does not (SILVA & SACEK, 2022).

One of the challenges in numerical modeling is to select the appropriate rheology for each layer since the reliability of the simulation highly depends on that. In this case, due to its significance, defining the rheology of the shear zones was a matter of great importance. MATOS *et al.* (2021) declares that the shear zones prevented and postponed the link between neighboring rift branches and accommodated early clockwise rotation. According to VAUCHEZ *et al.* (1995), the shear zones have a mylonitic composition and a sub-vertical orientation. Both statements lead to an interpretation that the shear zones behaved as rigid materials. As mentioned in the "inheritances section", this configuration allowed them to localize strain and not be torn apart during rifting. To best represent these zones we used upper crust rheology (see Table 4.1) with a scale factor $C = 1.4$.

Table 4.1 exhibits the values adopted in the numerical scenarios. The scale factor C is needed to deal with the magnitude of each defined parameter, i.e., increase or decrease their rheological contrasts when comparing to each other (SACEK, 2017). The shear zones and the Proterozoic Terranes have the same rheological parameters as the upper crust, but with different C values. The modified mantle has the rheology of the lithospheric mantle with a different C factor. Changes of the scale factor will be addressed in the results section when necessary.

A limitation imposed by our numerical models is that every layer has homogeneous rheology, which does not occur in nature and favors the development of perfectly symmetric rifts, also implausible. In order to avoid it, we used a random perturbation of the initial strain in each finite element of the model, as seen in the work of SILVA & SACEK (2022) and BRUNE *et al.* (2014). Here, the mean initial strain is 0.3 with a standard deviation of ≈ 0.08.

As the strain is randomly distributed across the domain, we can ensure the localization of strain in a certain spot by applying a weak seed (e.g., HUISMANS & BEAUMONT, 2003; SILVA & SACEK, 2022). In this work, as we want to assess the role of the inheritances in the rifting processes, we did not define a specific seed.

Therefore, in order to not influence too much the rifting positioning (i.e., let the location be random), every layer, except the asthenosphere, shear zones, and sticky air, represent a big seed.

Table 4.1: Rheological parameters used in the numerical scenarios. ρ is the reference density, A is the pre-exponent constant, Q is the activation energy, n is the exponent of the power law, V is the activation volume, H is the radiogenic heat production, C is the reference scale factor. Changes in the C value will be addressed in the results when necessary. These parameters follow the work of SILVA & SACEK (2022). Olivine data is from KARATO & WU (1993) and quartz data is from GLEASON & TULLIS (1995).

	Sticky Air	**Upper Crust**	**Lower Crust**	**Lithospheric Mantle**	**Asthenosphere**
Creep flow law	-	Quartz	Quartz	Dry olivine	Wet olivine
ρ (kg/m)	1	2700	2800	3354	3378
A (Pa^{-n}/s)	1.0×10^{-18}	8.574×10^{-28}	8.574×10^{-28}	2.4168×10^{-15}	1.393×10^{-14}
Q (kJ/mol)	0	222	222	540	429
n	1	4	4	3.5	3
V (m/mol)	0	0	0	25×10^{-6}	15×10^{-6}
H (W/Kg)	0	9.26×10^{-10}	2.86×10^{-10}	9.0×10^{-10}	0
C	0	1	1	0.8	1

Table 4.2: Fixed parameters for the numerical scenarios. Data from SILVA & SACEK (2022).

Parameter	**Description**	**Value**
α	Volumetric expansion coefficient	3.28×10^{-5} K^{-1}
κ	Thermal diffusivity	10^{-6} m^2/s
c_p	Specific heat capacity	1250 J/kg/K
x_σ	Half-width for the denudation function	32.5 km
x_c	Position of maximum denudation	260 km
k_{sp}	Maximum denudation rate	8×10^{-4} m/year
h_{sl}	Sea level relative to the initial altitude	-1000 m

Chapter 5

Results

The numerical models of this work simulate the rifting of a two-dimensional, layered Earth during 30 Myr with an extension rate of 2.0 mm/year (some cases have an extension of 1.6 mm/year and will be properly indicated). In the following sections, we show the accumulated strain and the viscosity plots for selected deformation stages and scenarios.

In this chapter, the terms "coupled" and "decoupled lithosphere" are used as a reference to the degree of coupling between the lithospheric mantle and the upper crust. These oversimplified terms are for ease of reading and comprehension, as both "coupled" and "decoupled" scenarios have a certain degree of coupling (e.g., SILVA & SACEK, 2022).

Additionally, the models are separated into two primary categories based on the rheology of the modified lithospheric mantle (Fig. 4.2). Firstly, we modeled a depleted modified mantle, meaning a mantle with rigid rheology following GANADE *et al.* (2021). Afterward, we considered a fertilized mantle consistent with the model proposed by CHENIN *et al.* (2019).

5.1 Scenario 0: Reference model

Initially, we present the result of the reference model, that is, the most simple scenario, where we did not include a modified lithospheric mantle beneath the fragile Tonian Terranes (i.e., Cachoeirinha-Seridó and Cariris Velhos; GANADE *et al.*, 2021) because we wanted to analyze the role of the crustal inheritances alone and a modified mantle below them would modify our assessment. In this case, we assumed a homogeneous lithospheric mantle, without lateral variations of rheological properties.

In the upper crust, the terranes have the same rheological parameters of the adjacent crustal blocks, but with $C = 0.8$ (Table 5.1). It means that the viscosity

Table 5.1: Rheological parameters adopted in the Reference Model that differ from the regular parameters shown in Table 4.1. The parameters adopted for each reference interface can be seen in Table 4.1. See the numerical interfaces in Fig. 4.2 for a better understanding of the distribution and location of the layers. This scenario has an extension rate of 2.0 mm/year.

Layer	**Reference layer**	C
Lower Crust (Proterozoic Terranes)	Upper Crust	0.8
Upper Crust (Proterozoic Terranes)	Upper Crust	0.8

of these terranes is 80% of the upper crust with $C = 1$ at the same temperature, pressure, and strain rate (e.g., SILVA & SACEK, 2022).

Fig. 5.1 exhibits how an inherited fragile terrane affects the extensional deformation. The weaker rheology of the Cachoeirinha-Seridó and Cariris-Velhos terranes controlled the rift localization and strain distribution in a way that no faulting was developed on the "normal" Paleoproterozoic Borborema crust (see fig. 2.2 for age reference). Geological cross-sections (Fig. 2.2) show that there are no major basins in these terranes, such as the rifting seen in the model, hence there may exist a geological factor that prevented the formation or large rifts in this area.

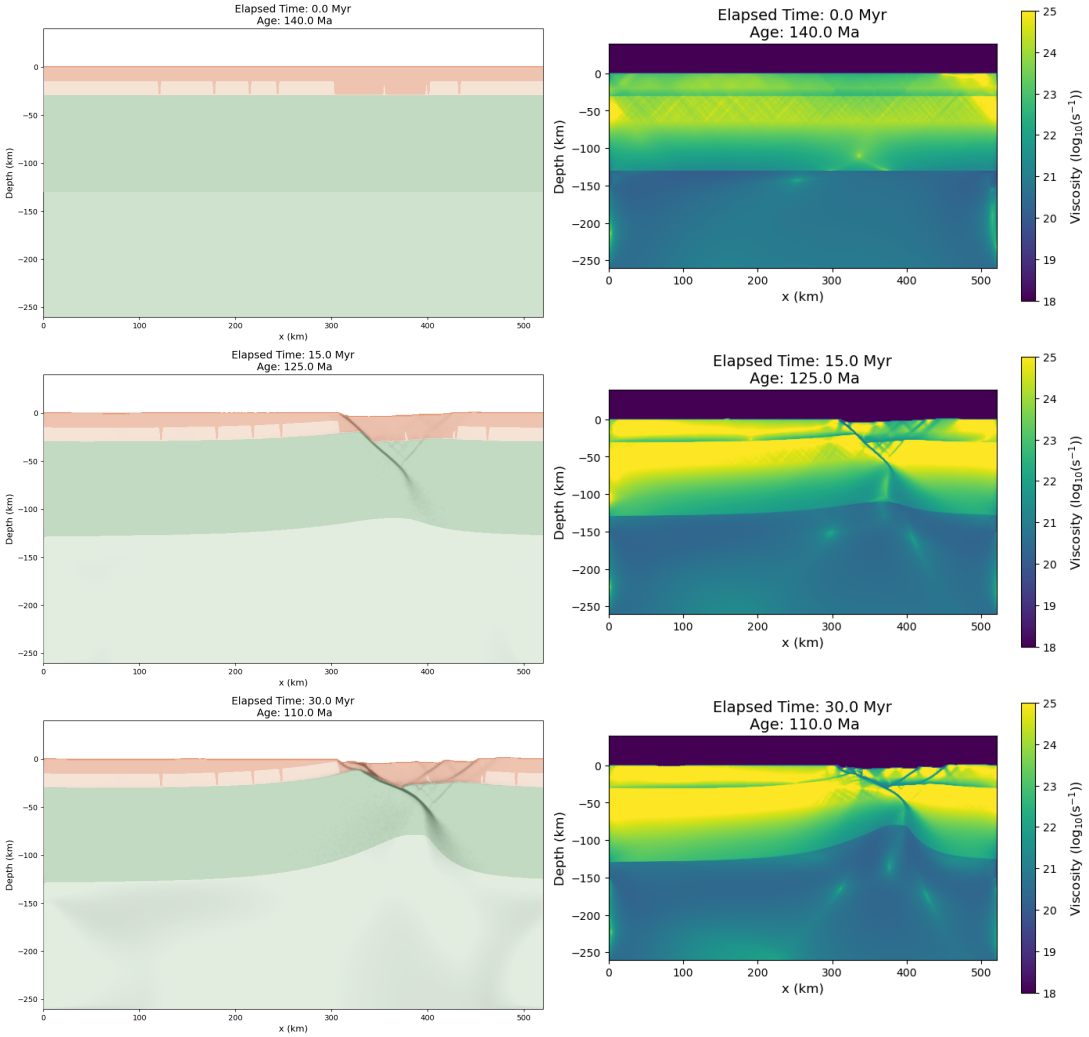

Figure 5.1: Accumulated strain (left) and viscosity plots (right) for the Reference Model, i.e., with fragile Proterozoic terranes and no strong lithospheric mantle beneath them. Dark and light orange represent the upper and lower crust, respectively. The vertical, thin, dark orange structures represent the shear zones, and the dark orange rectangular structure represents the Proterozoic Terranes. Dark and light green represent the lithospheric and sublithospheric mantle, respectively. Shades of gray correspond to the accumulated strain.

5.2 Scenarios with a rigid modified mantle (RM)

5.2.1 RM1: rigid mantle 1

In this model, we added a strong mantle beneath the Proterozoic Terranes with the same width as the Tonian terranes above (Fig. 4.2). This layer has the same rheological parameters of the lithospheric mantle, but with $C = 1.4$ (Table 5.2). The introduction of this layer is based on the work of GANADE *et al.* (2021) that was previously explained in the inheritances section.

Fig. 5.2 shows that no faulting was developed in the depleted mantle due to its rigid rheology (viscosity plots show that the higher viscosity zone, i.e., the depleted mantle, remained intact), which does not occur in the reference model (Fig. 5.1).

Table 5.2: Rheological parameters adopted in the Model RM1 that differ from the regular parameters shown in Table 4.1. The parameters adopted for each reference interface can be seen in Table 4.1. See the numerical interfaces in Fig. 4.2 for a better understanding of the distribution and location of the layers. This scenario has an extension rate of 2.0 mm/year and a 'thin' Modified Lithospheric Mantle.

Layer	**Reference layer**	C
Modified Lithospheric Mantle	Lithospheric Mantle	1.4
Lower Crust (Proterozoic Terranes)	Upper Crust	0.8
Upper Crust (Proterozoic Terranes)	Upper Crust	0.8

The rheology of the Cachoeirinha-Seridó belt and the Cariris-Velhos terrane still controlled the rifting. Part of the necking zone happened in the transition from the rigid to the "soft" lithospheric mantle, indicating that the deformation finds a way towards the weaker region.

In accordance with the reference model, an asymmetric rift was developed in the Proterozoic Terranes. Also, in both scenarios, the lower crust of the Terranes is slightly less viscous ($C = 0.8$) than the adjacent, regular lower crust ($C = 1$). That is, the coupling between the mantle and the upper crust in this zone is weaker.

5.2.2 RM2: augmented coupling of the lower Proterozoic Terranes

In this model, we increased the viscosity of the lower crust of the fragile Proterozoic Terranes, such as the coupling of its upper part with the depleted lithospheric mantle below, by adopting $C = 1.4$ (Table 5.3).

Table 5.3: Rheological parameters adopted in the Model RM2 that differ from the regular parameters shown in Table 4.1. The parameters adopted for each reference interface can be seen in Table 4.1. See the numerical interfaces in Fig. 4.2 for a better understanding of the distribution and location of the layers. This scenario has an extension rate of 2.0 mm/year and a 'thin' Modified Lithospheric Mantle.

Layer	**Reference layer**	C
Modified Lithospheric Mantle	Lithospheric Mantle	1.4
Lower Crust (Proterozoic Terranes)	Upper Crust	1.4
Upper Crust (Proterozoic Terranes)	Upper Crust	0.8

The higher viscosity of both lower Terranes and the underlying mantle prevented the Cachoeirinha-Seridó and Cariris Velhos belts from faulting, which moved the rift axis away from it, to the left (Fig. 5.3). The graben formed in the Paleoproterozoic

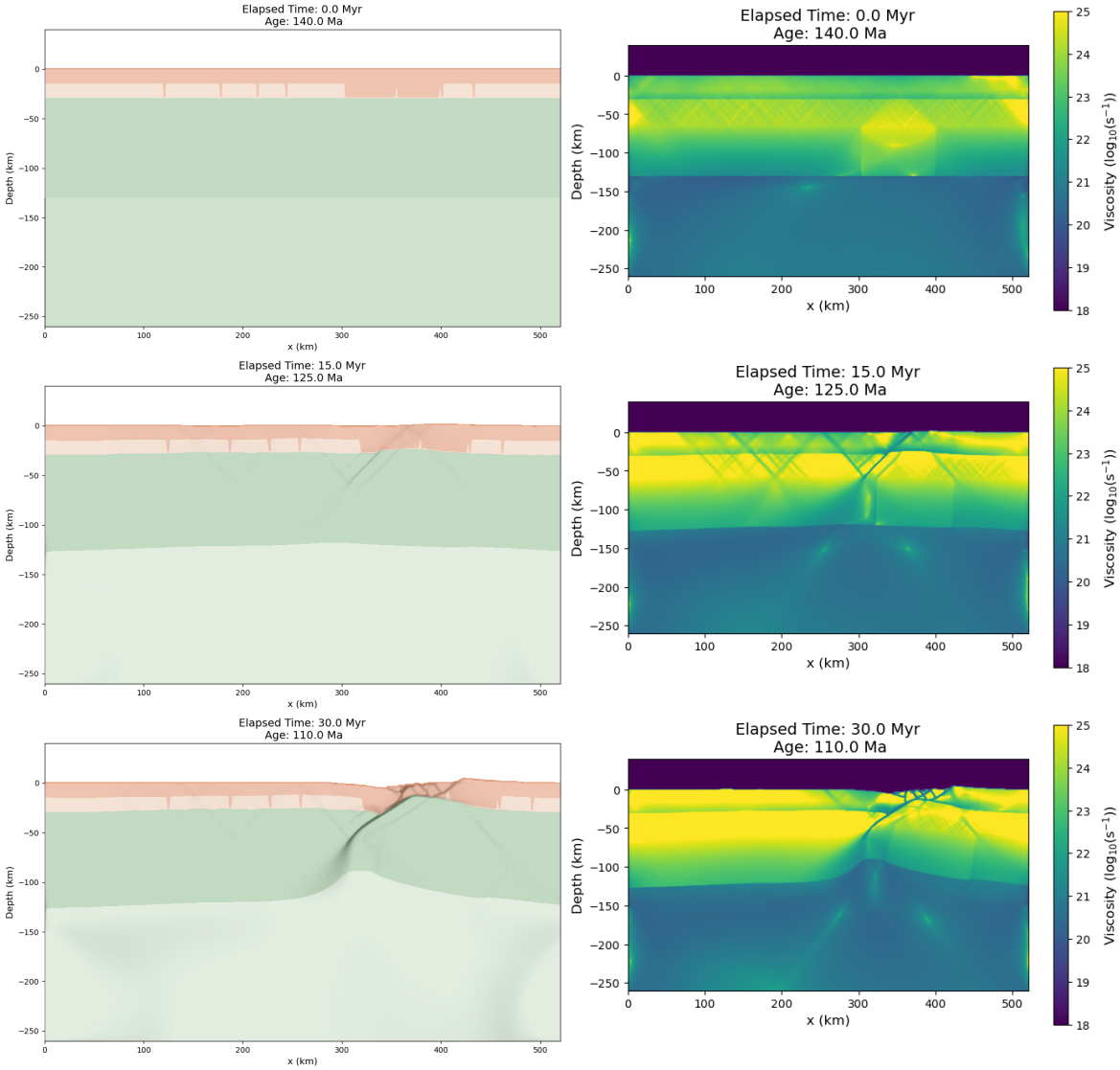

Figure 5.2: Accumulated strain (left) and viscosity plots (right) for the RM1 scenario, which main features are the fragile Proterozoic terranes and the strong lithospheric mantle beneath them. Dark and light orange represent the upper and lower crust, respectively. The vertical, thin, dark orange structures represent the shear zones, and the dark orange rectangular structure represents the Proterozoic Terranes. Dark and light green represent the lithospheric and sublithospheric mantle, respectively. Shades of gray correspond to the accumulated strain.

Borborema basement assumed a more symmetric characteristic, which does not agree with the rift geometry of the intracontinental basins in NE Brazil (MATOS, 1999, 1992; MATOS *et al.*, 2021).

The shear zones did not perform any major role in this scenario, as we do not have faults nucleating from them (MATOS, 1999). Also, Fig. 5.3 shows that one of the zones got severed in the process, which should not occur.

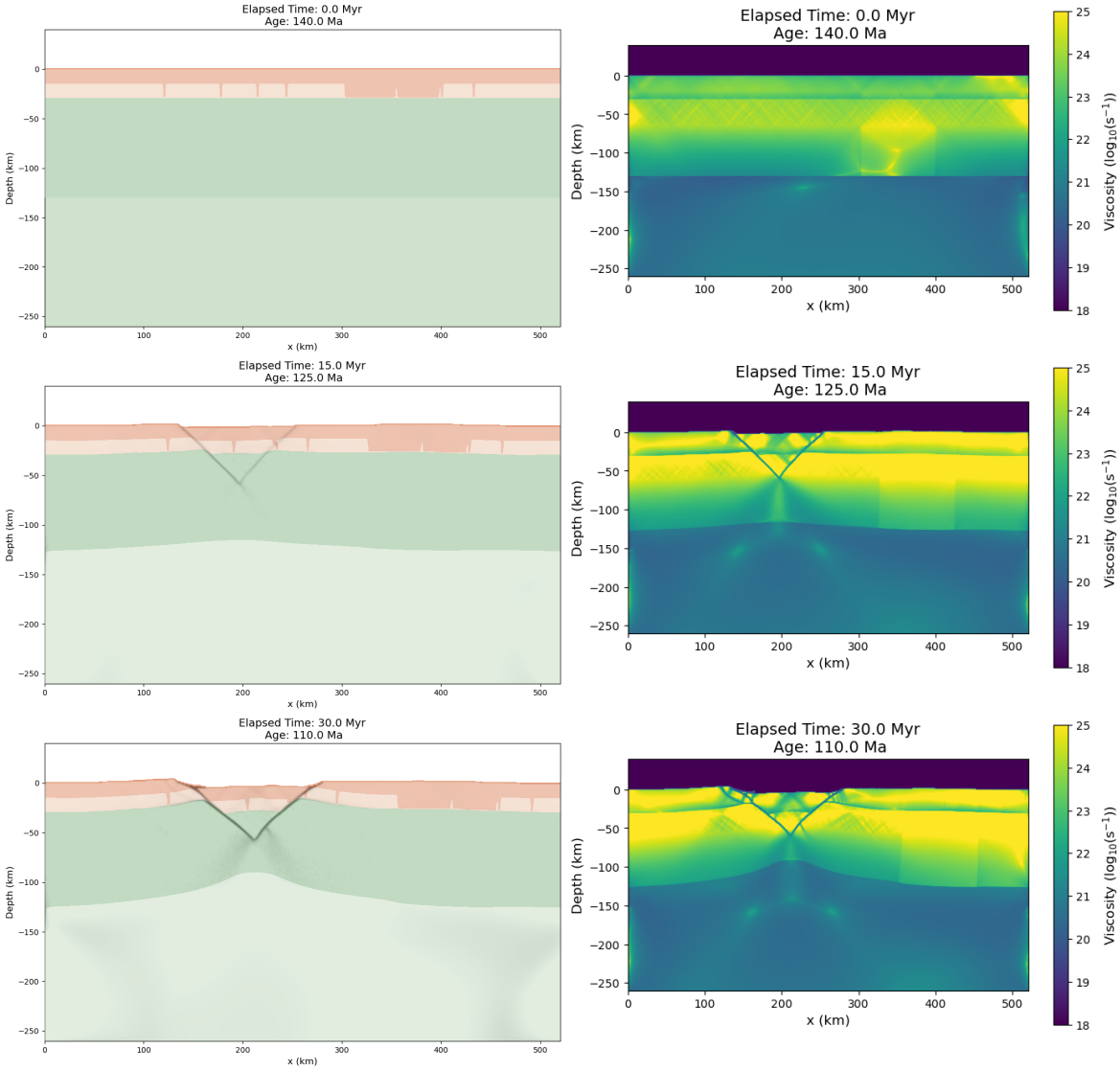

Figure 5.3: Accumulated strain (left) and viscosity plots (right) of the model RM2, which main characteristic is the addition of a higher viscosity lower crust beneath the Tonian Terranes. Dark and light orange represent the upper and lower crust, respectively. The vertical, thin, dark orange structures represent the shear zones, and the dark orange rectangular structure represents the Proterozoic Terranes. Dark and light green represent the lithospheric and sublithospheric mantle, respectively. Shades of gray correspond to the accumulated strain.

5.2.3 RM3: low viscosity lower crust

Fig. 5.4 illustrates the deformation of the crust with the fragile terranes and weak coupling between the lower crust and the lithospheric mantle. It is important to mention that the rheology of the lower Proterozoic Terranes is the same adopted in the scenarios 0 and RM1 (i.e., $C = 0.8$, Table 5.4).

This scenario adopted a less viscous lower crust in comparison with the previous model, $C = 0.5$. We can see that the decoupling between the crust and mantle affected the rifting style: faults were formed in the basement (not in the Proterozoic

Table 5.4: Rheological parameters adopted in the Model RM3 that differ from the regular parameters shown in Table 4.1. The parameters adopted for each reference interface can be seen in Table 4.1. See the numerical interfaces in Fig. 4.2 for a better understanding of the distribution and location of the layers. This scenario has an extension rate of 2.0 mm/year and a 'thin' Modified Lithospheric Mantle.

Layer	**Reference layer**	C
Modified Lithospheric Mantle	Lithospheric Mantle	1.4
Lower Crust	Lower Crust	0.5
Lower Crust (Proterozoic Terranes)	Upper Crust	0.8/1.4
Upper Crust (Proterozoic Terranes)	Upper Crust	0.8

terranes), and some shear zones were brittle reactivated (RAMOS *et al.*, 2022) at the same time they delimited the rifting area, which we should expect based on the work of MATOS (1999).

The weaker coupling between the upper crust and the lithospheric mantle of the "normal" Borborema basement is even weaker if compared to the coupling of the Proterozoic Terranes. This setting allowed the localization of the rift axis away from the fragile terranes, which were previously controlling the rifting. During the lithospheric stretching, the lower crust flowed laterally, which allowed the formation of an asymmetric rift with its half-graben relief (Fig. 5.4). Also, synthetic and antithetic faults are seen spreading away from the main faults.

We also have a version of this scenario in which the lower Proterozoic Terranes has the same rheology as the one adopted in RM2 ($C = 1.4$; Model RM3b). The result obtained (Fig 5.5 is very similar to the previous one, indicating that rheology of the lower crust, that is, the coupling between the upper crust and the lithospheric mantle is a significant parameter in this type of rifting. Here, the upper crust structures did not define the onset of rifting, they just controlled the continuation of it after it had already started.

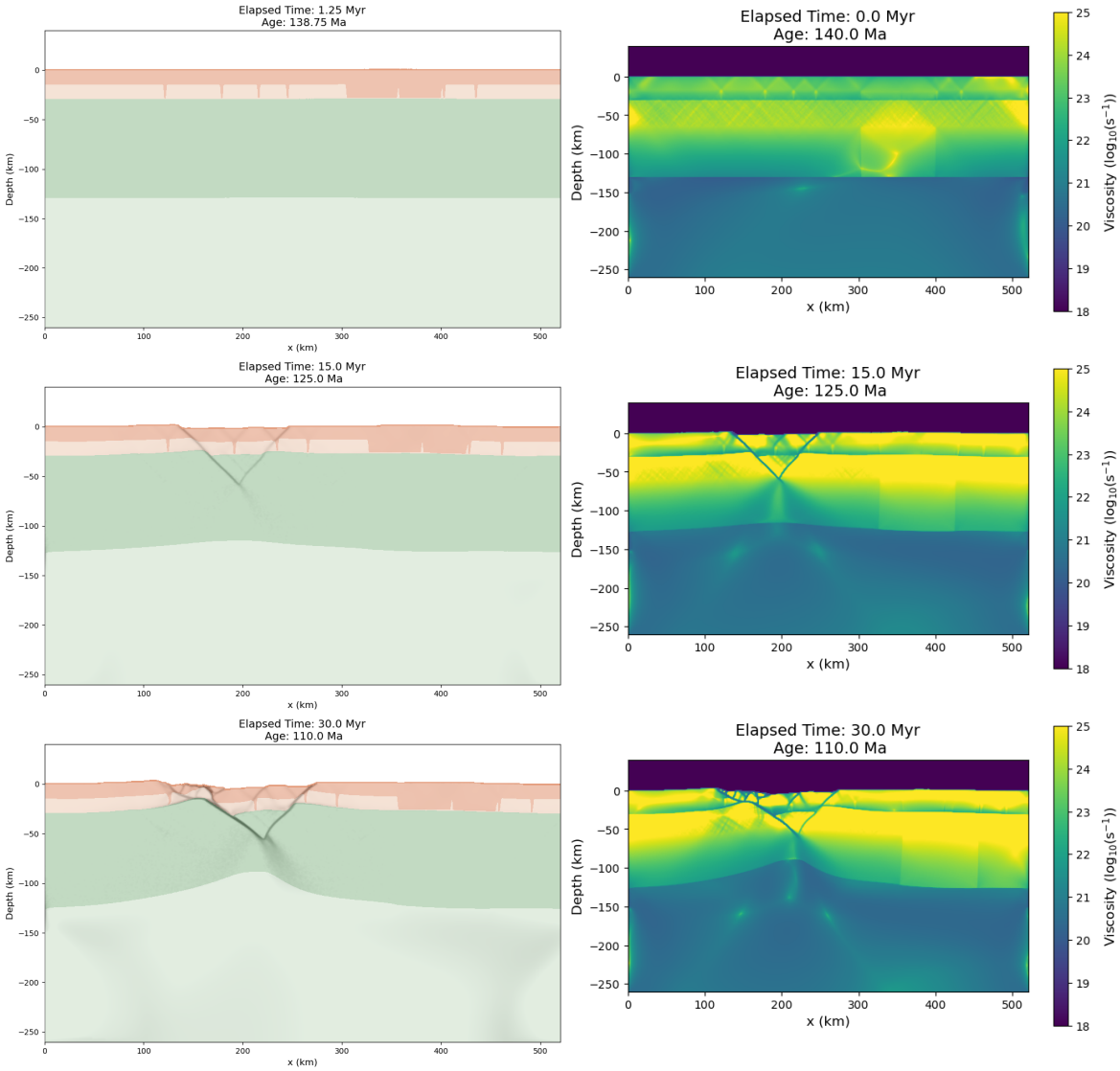

Figure 5.4: Accumulated strain (left) and viscosity plots (right) of the Model RM3a. Dark and light orange represent the upper and lower crust, respectively. The vertical, thin, dark orange structures represent the shear zones, and the dark orange rectangular structure represents the Proterozoic Terranes. Dark and light green represent the lithospheric and sublithospheric mantle, respectively. Shades of gray correspond to the accumulated strain.

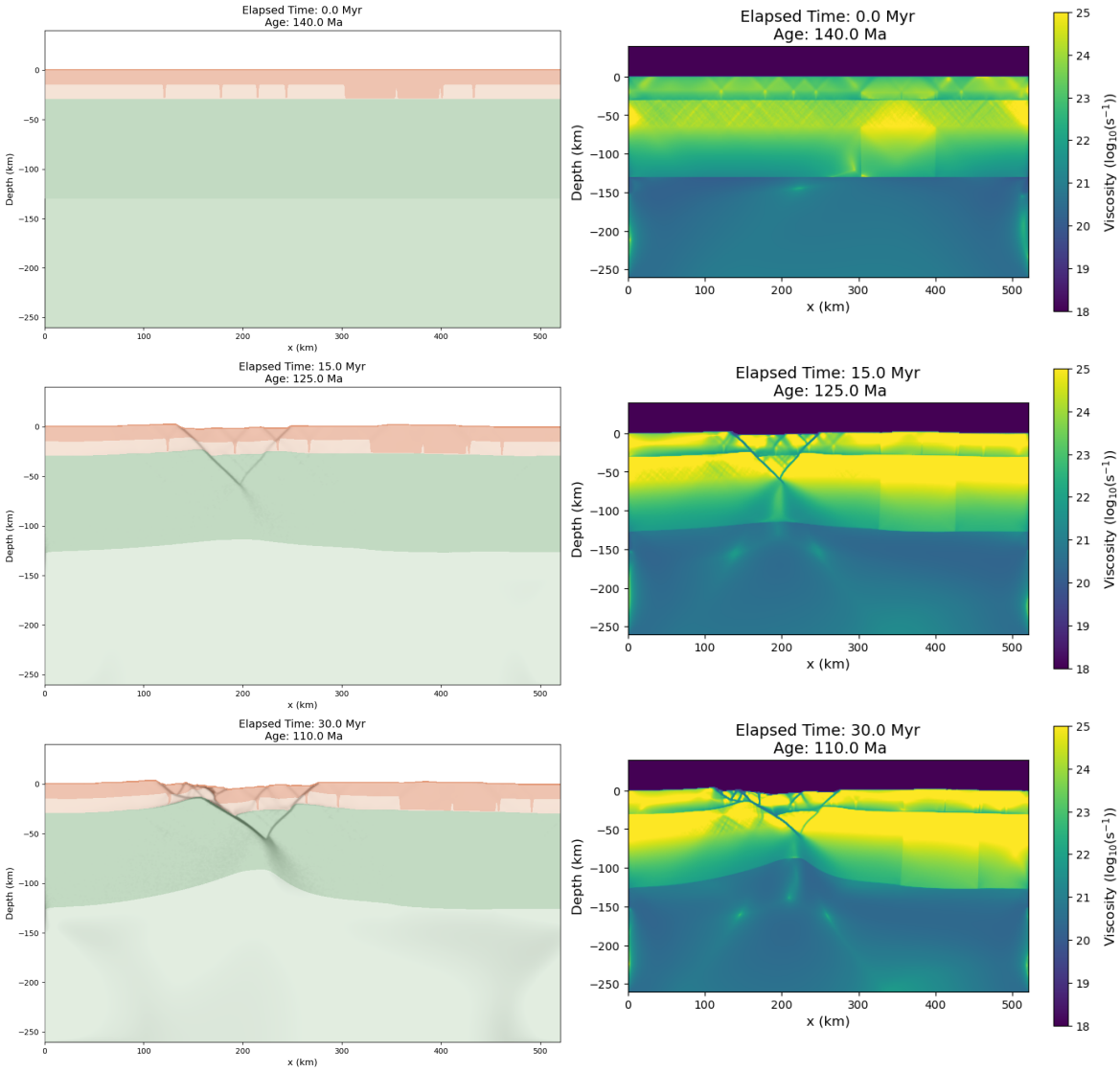

Figure 5.5: Accumulated strain (left) and viscosity plots (right) of the Model RM3b. Dark and light orange represent the upper and lower crust, respectively. The vertical, thin, dark orange structures represent the shear zones, and the dark orange rectangular structure represents the Proterozoic Terranes. Dark and light green represent the lithospheric and sublithospheric mantle, respectively. Shades of gray correspond to the accumulated strain.

5.3 Scenarios with a fragile modified mantle (FM)

5.3.1 FM1: low viscosity lower crust

This scenario has the same rheological parameters as Model RM3b, except for the modified mantle ($C = 0.5$; Table 5.5). Here, we adopted the fertilized, weak rheology pointed out by CHENIN *et al.* (2019). Fig. 5.6 illustrates the deformation of the crust with a fragile mantle underneath the Proterozoic Terranes.

Table 5.5: Rheological parameters adopted in the Model FM1 that differ from the regular parameters shown in Table 4.1. The parameters adopted for each reference interface can be seen in Table 4.1. See the numerical interfaces in Fig. 4.2 for a better understanding of the distribution and location of the layers. This scenario has an extension rate of 2.0 mm/year and a 'thin' Modified Lithospheric Mantle.

Layer	**Reference Layer**	C
Modified Lithospheric Mantle	Lithospheric Mantle	0.5
Lower Crust	Lower Crust	0.5
Lower Crust (Proterozoic Terranes)	Upper Crust	1.4
Upper Crust (Proterozoic Terranes)	Upper Crust	0.8

Here, for the first time, the rift was formed in the expected location of the Araripe Basin (see the cross-sections in Fig. 2.2). The rift nucleation is primarily controlled by the fragile portion of the lithospheric mantle, while the crustal heterogeneities play a secondary role. The shear zones were brittle reactivated after the necking and onset of rifting, delimiting the basin area (MATOS, 1999; RAMOS *et al.*, 2022).

The topographic evolution indicates a more symmetric rift with both shoulders exhibiting similar geometries, levels, and dip. Also, the whole rift displays a strong relief , marked by a steep escarpment with no pronounced half-grabens as expected.

5.3.2 Scenarios with a wide modified mantle

The Sm-Nd T_{DM} age map and the P-wave tomography model for the Borborema Province in figure 2.1 exhibit the heterogeneity caused by the different composition of the modified lithospheric mantle. This feature extends from the Pernambuco Shear Zone (PE) to the subsidiary shear zone above Patos (PA), different from what we adopted in the previous models. Therefore, in the following scenarios, a wider modified mantle was chosen. Fig. 4.2 exhibits the width of the wide modified mantle.

Furthermore, the scenarios below have an extension rate of 1.6 mm/year, slower than the ones seen previously, and have the same rheological parameters, except

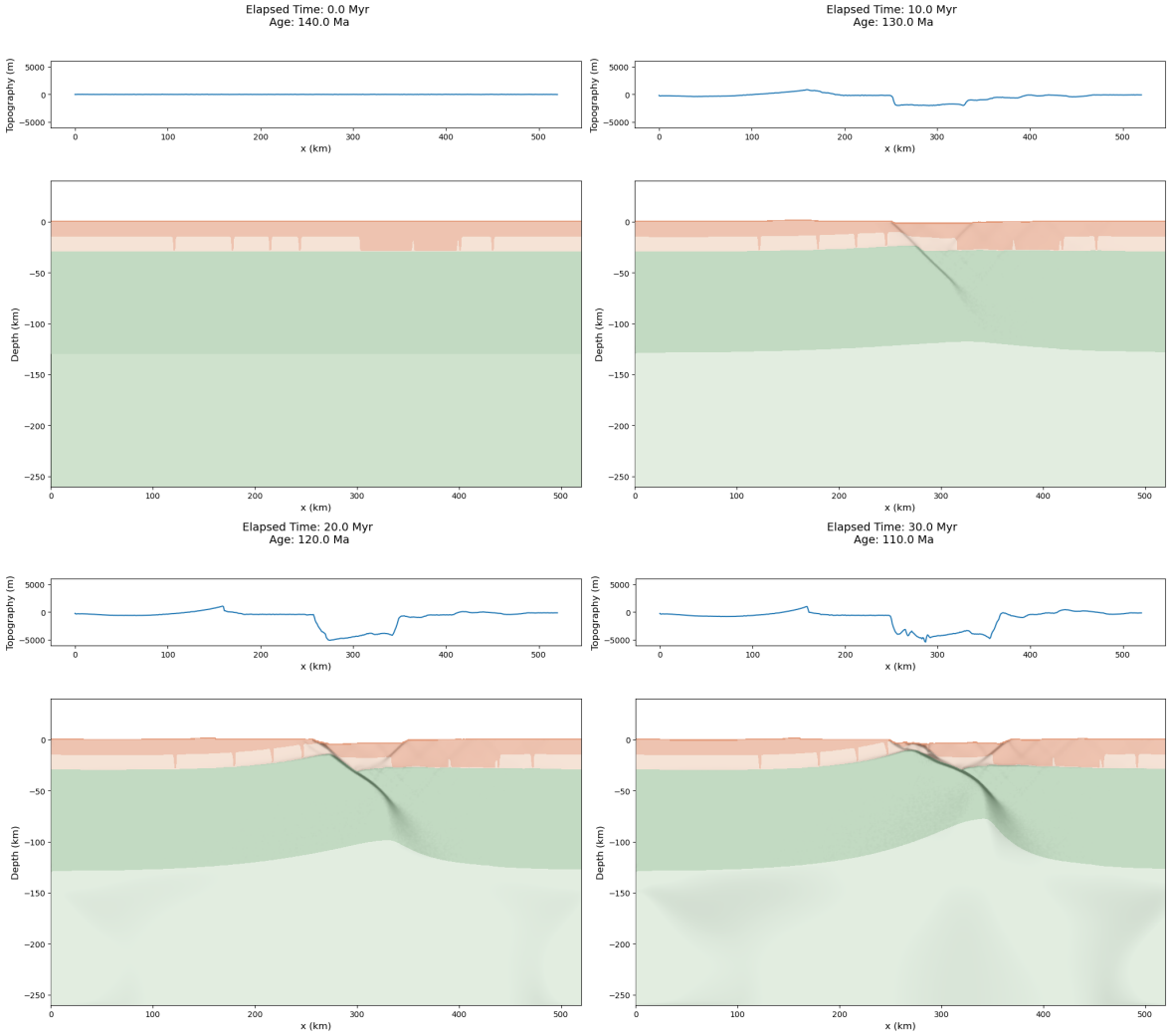

Figure 5.6: Accumulated strain, and topographic plots of the Model FM1. Dark and light orange represent the upper and lower crust, respectively. The vertical, thin, dark orange structures represent the shear zones, and the dark orange rectangular structure represents the Proterozoic Terranes. Dark and light green represent the lithospheric and sublithospheric mantle, respectively. Shades of gray correspond to the accumulated strain.

by the viscosity of the lower crust. The adopted C factor for the interfaces follows Table 4.1, with some exceptions: the modified mantle (Fig. 4.2) has $C = 0.5$, and the lithospheric mantle has $C = 1.4$, in order to create a rheological contrast. We kept the high viscosity of the lower crust of the Proterozoic Terranes ($C = 1.4$). Differences in the C factor of the lower crust will be addressed in each case.

FM2: weak crust-mantle coupling

In this model, we adopted $C = 0.5$ for the lower crust in order to assess its impact during rifting. Table 5.6 summarizes the main differences of the C factors in comparison to the reference rheological parameters in Table 4.1.

Fig. 5.7 shows that the location of the necking zone is formed in the region with

Table 5.6: Rheological parameters adopted in the Model FM2 that differ from the regular parameters shown in Table 4.1. The parameters adopted for each reference interface can be seen in Table 4.1. See the numerical interfaces in Fig. 4.2 for a better understanding of the distribution and location of the layers.

Interface	**Reference interaface**	C
Lithospheric Mantle	Lithospheric Mantle	1.4
Modified Lithospheric Mantle	Lithospheric Mantle	0.5
Lower Crust	Lower Crust	0.5
Lower Crust (Proterozoic Terranes)	Upper Crust	1.4
Upper Crust (Proterozoic Terranes)	Upper Crust	0.8

weak mantle, and close to the boundary with the non-modified lithosphere. Towards the end of the simulation, the faults extend to the Tonian Terranes, forming smaller and shallower basins in comparison to the one in the main graben. This agrees with the geological cross-sections shown in Fig. 2.2.

In addition, as observed in previous models, the shear zones play a secondary role in the rifting processes. The rift nucleation is primarily defined by the location of weak layers in the lithoshere, while the crustal inheritances are activated later, after the onset of rifting and work delimiting the rifting area.

The topographic evolution indicates a more symmetric rift with both shoulders exhibiting similar geometries, levels, and dip. Also, as seen in previous scenarios, the whole rift displays a strong relief marked by a steep escarpment with no pronounced half-grabens as expected.

FM3: strong crust-mantle coupling

In this model, different from the previous one, we adopted $C = 1.0$ for the lower crust, which increased the degree of coupling between the upper crust and the lithospheric mantle. Table 5.7 summarizes the main differences of the C factors in comparison to the reference rheological parameters in Table 4.1.

Fig. 5.8 shows very similar results to those obtained in model FM2. The location of the necking zone is formed in the region with a weak mantle, and close to the boundary with the non-modified lithosphere. Towards the end of the simulation, the faults extend to the Tonian Terranes, forming smaller and shallower basins in comparison to the one in the main graben. This agrees with the geological cross-sections shown in Fig. 2.2.

Here, as indicated by the topographic evolution (Fig. 5.8), we have a relief marked by steep fault planes and a symmetric basin. The higher degree of coupling directly influences the strain distribution on the model (BUROV *et al.*, 2006), which

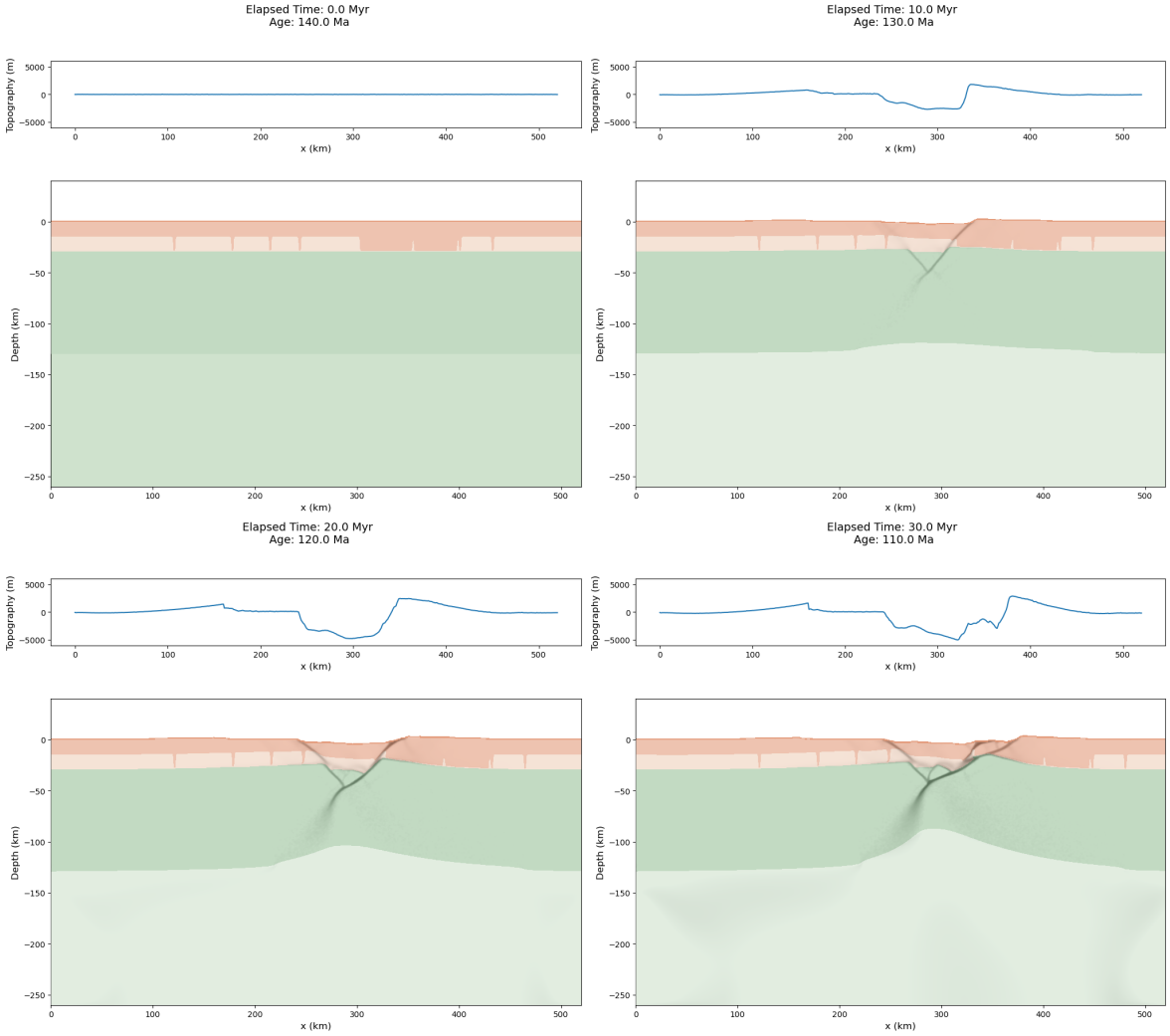

Figure 5.7: Accumulated strain, and topographic plots of the Model FM2. Dark and light orange represent the upper and lower crust, respectively. The vertical, thin, dark orange structures represent the shear zones, and the dark orange rectangular structure represents the Proterozoic Terranes. Dark and light green represent the lithospheric and sublithospheric mantle, respectively. Shades of gray correspond to the accumulated strain.

Table 5.7: Rheological parameters adopted in the Model FM3 that differ from the regular parameters shown in Table 4.1. The parameters adopted for each reference interface can be seen in Table 4.1. See the numerical interfaces in Fig. 4.2 for a better understanding of the distribution and location of the layers.

Interface	**Reference interaface**	C
Lithospheric Mantle	Lithospheric Mantle	1.4
Modified Lithospheric Mantle	Lithospheric Mantle	0.5
Lower Crust	Lower Crust	1.0
Lower Crust (Proterozoic Terranes)	Upper Crust	1.4
Upper Crust (Proterozoic Terranes)	Upper Crust	0.8

substantially changes how a rift nucleates.

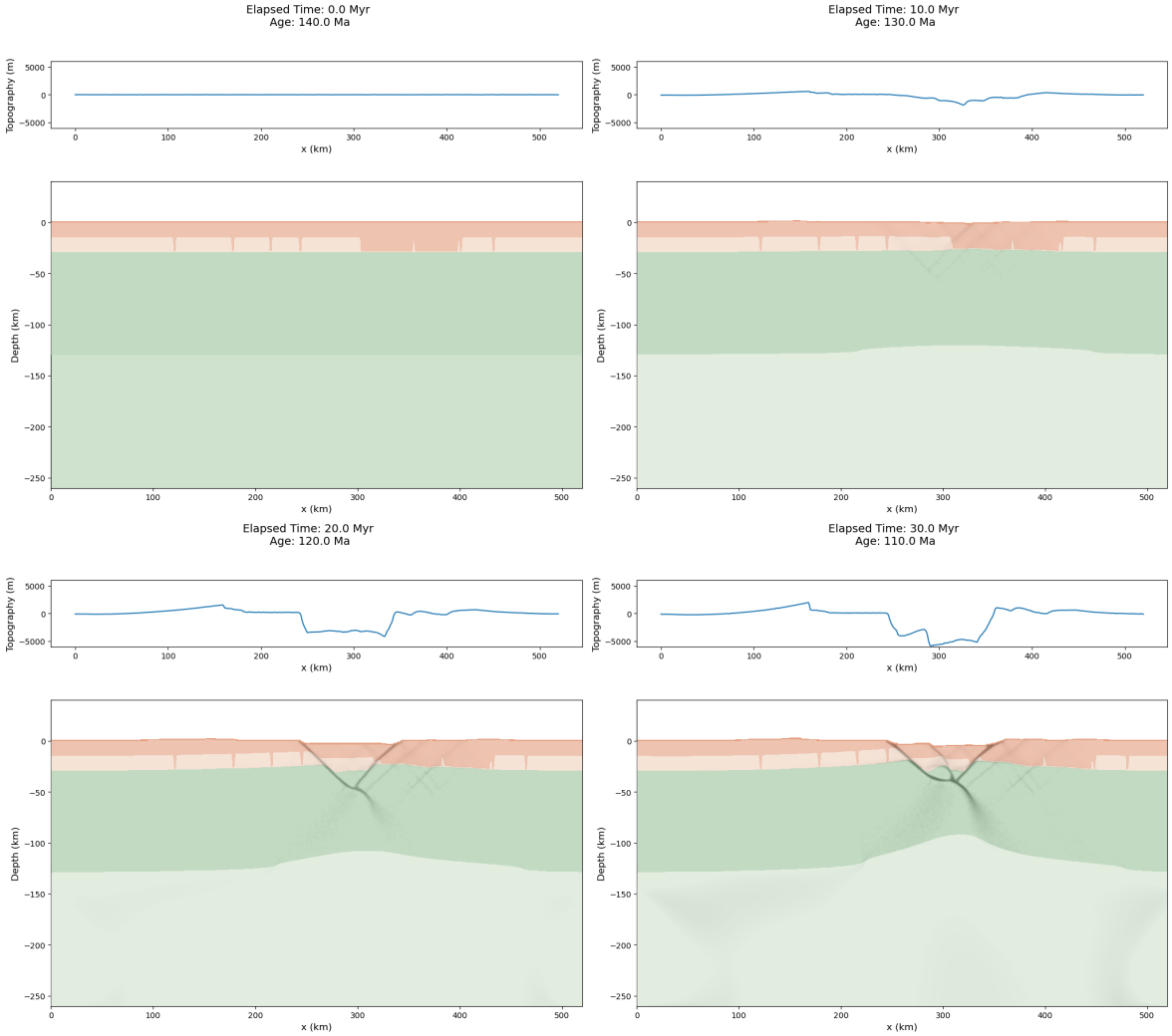

Figure 5.8: Accumulated strain, and topographic plots of the Model FM3. Dark and light orange represent the upper and lower crust, respectively. The vertical, thin, dark orange structures represent the shear zones, and the dark orange rectangular structure represents the Proterozoic Terranes. Dark and light green represent the lithospheric and sublithospheric mantle, respectively. Shades of gray correspond to the accumulated strain.

Chapter 6

Discussion

6.1 The role of inheritances in controlling lithospheric dynamics

Examples of rifting controlled by preexisting structures are seen worldwide (e.g., CORTI *et al.*, 2007; NYBLADE & BRAZIER, 2002; RING, 1994). In Brazil, the main examples are those of the Borborema Province (e.g., MATOS, 1992; MATOS *et al.*, 2021; NOGUEIRA *et al.*, 2015; RAMOS *et al.*, 2022) due to their "inherited past".

Much is debated that brittle reactivation of Precambrian shear zones in northeastern Brazil has accommodated deformation in the interior of West Gondwana during the rifting of the South Atlantic (GANADE *et al.*, 2022; MATOS, 2000, 1999, 1992; MATOS *et al.*, 2021; MILANI & DAVISON, 1988; ROSA *et al.*, 2023). Actually, works based on field and geophysical data show a relation between Proterozoic shear zones and boundary faults (e.g., GANADE *et al.*, 2022; NOGUEIRA *et al.*, 2015; RAMOS *et al.*, 2022).

However, the timing of the reactivation - which may really define the role of these structures in controlling basin evolution - is still uncertain due to a lack of data. By timing here, we mean the age relative to mantle uplifting and doming of the upper crust. Based on U-Pb dating of carbonates, GANADE *et al.* (2022), MIRANDA *et al.* (2020), and LOPES *et al.* (2019) confirm brittle reactivation of the shear zones during the Cretaceous with NE-SW shortening and NW-SE extension.

The complex evolution of the Borborema Province (ARTHAUD *et al.*, 2008; GANADE *et al.*, 2014, 2021; VAN SCHMUS *et al.*, 2011, and references therein) superimposed weak layers atop strong structures and connected contrasting lithologies. Although being weak terranes (see the inheritances section; GANADE *et al.* 2021), the Cariris Velhos and Cachoeirinha Seridó belts did not localize the rifting axis. It occurred when we did not consider a strong lower crust beneath them

(scenarios 0 and RM1).

Our scenarios show that upper crust structural inheritances do not have a significant impact on controlling the localization and formation of a rift on their own (e.g., reference model, Fig. 5.1). They may be really relevant on local scales, but regarding lithospheric dynamics, the mantle (and lower crust) rheology and structure are the leading actors (e.g., CHENIN & BEAUMONT, 2013; CHENIN *et al.*, 2019; MANATSCHAL *et al.*, 2015) (Figs. 5.4, 5.6, 5.7, 5.8).

The Rift commenced and was controlled by the lower crust and lithospheric mantle, and thereafter was bounded by the upper crust structures. The degree of coupling between the upper crust and the lithospheric mantle defines the efficiency of stress distribution from the mantle to the layers above (BUROV *et al.*, 2006).

These results add up to other models that demonstrate rifting location occurs in weak layers within the lithosphere, and that mantelic heterogeneities have a major role in strain localization when compared to crustal heterogeneities (e.g., ALESSANDRO *et al.*, 2023; CHENIN & BEAUMONT, 2013; CHENIN *et al.*, 2019; MANATSCHAL *et al.*, 2015).

To conclude, we have seen that the scenarios with the fragile (fertilized) mantle, as indicated by CHENIN *et al.* (2019) produced a more reliable result when comparing to the present-day distribution, and localization of the Mesozoic basins. We suggest that the lateral heterogeneity of the lithospheric mantle is a main driver for rift nucleation. This means that the contact of portions with different degrees of rigidity creates boundary effects for the nucleation of plastic deformations.

6.2 Topographic evolution and provenance implications

The Araripe Basin is the largest Mesozoic intracontinental basin in the Cariri Valley and northeastern Brazil. Its main phase of sedimentation started in the Early Cretaceous during the rift and lasted until the mid-Aptian under a stable post-rift setting (ASSINE, 1992, 2007, and references therein). The sedimentation is predominantly composed of fluvial-lacustrine beds with abundant and well-preserved fossils, which suggests a connection to the Tethyan fauna/flora (ARAI, 2014).

The connection with the Tethyan Sea during the basin development is a topic widely accepted by the academic community due to the irrefutable fossiliferous content (ARAI, 2014, 2016; MAISEY, 2000, and references therein). Notwithstanding, there is a great debate regarding the direction in which this connection was achieved, that is, whether it occurred through the Parnaíba Basin on the N-NW (ARAI, 2014; SOUZA *et al.*, 2022, and references therein), through the Potiguar Basin on the NE

(KROTH *et al.*, 2021, and references therein), or even from the S-SW through the Reconcavo-Tucano-Jatobá rift (ASSINE, 2007; ASSINE *et al.*, 2014).

SOUZA *et al.* (2022) performed U-Pb analysis in 10 sandstone samples from all supersequences of the Araripe Basin, along with paleocurrent, stratigraphic and structural data, to assess the sedimentary provenance of the basin. Six provenance patterns were identified, which indicate rapid changes in the tectono-sedimentary evolution of the NE intracontinental basins.

The paleogeographic scenarios postulated by SOUZA *et al.* (2022) show that, initially, during the Late Jurassic, a topographic high formed by the Paleozoic-Triassic sedimentary rocks of the Parnaíba Basin was the sediment source to the Araripe. In the late-Aptian, depression on Rio Salgado Belt, NE of Araripe, allowed the connection of the Cariri with the Potiguar Basin, and thus, the first marine incursions (SOUZA *et al.*, 2022).

Also, lithogeochemistry data from clay samples of the Aptian Crato Member, Araripe Basin, indicate provenance from post-Archean intermediate rocks, and sudden salinity increases due to marine influence, that is, the connection with the new ocean at the Equatorial Atlantic Margin (SALGADO-CAMPOS *et al.*, 2021).

The numerical scenarios with a thin lithospheric mantle, excluding those which the necking occurred in the Tonian Terranes, show that the asymmetric rifting was responsible for creating topographic highs to the NW of the Cariri Valley, such as depressions in the central area that may extend to NE and SW (Figs. 5.4, 5.5). This whole topographic configuration sets up an ideal environment for marine incursions coming from the northeast (SOUZA *et al.*, 2022), which eroded the felsic basement and the intermediate rocks of the Cachoeirinha-Seridó and Cariris-Velhos belts.

However, according to SOUZA *et al.* (2022), the topographic highs surrounding the Cariri-Valley were not decisive for the marine incursion in the late-Aptian times, but the mentioned depression in the central Transversal Zone. Therefore, the wide (and fragile) mantle scenarios, which does not show a pronounced asymmetric topography can still support the hypothesis of marine incursion coming from the NE. It is worth mentioning that the adopted extension rates may have a significant impact on the topographic evolution of the region, so future simulations with a more adjusted velocity field may exhibit a different or, at least, a less pronounced relief.

6.3 How may lithospheric inheritances affect a sedimentary basin's economic potential?

The Cariri Valley basins, especially the Araripe, have no economic potential for regular hydrocarbon production. Although their organic content is composed of

Type I kerogen - a good quality matter associated with the generation of abundant amounts of oil - the burial was not enough to maturate the organic matter (ASSINE, 2007; FAMBRINI *et al.*, 2020; NEUMANN *et al.*, 2003; SPIGOLON *et al.*, 2015).

Post-rift inversion of the Cariri basins (RICHETTI *et al.*, 2022, and references therein) also had an impact on the maturation of the organic matter. According to MORAIS NETO *et al.* (2006), the post-rift inversion of the basin ceased the thermal maturity of its organic matter, compromising its hydrocarbon generation.

As seen in the numerical scenarios, the coupling between the lower crust and the lithospheric mantle affects the distribution of strain throughout the crust and, therefore, the depth of the rift valleys. Coupled scenarios tend to produce more localized, symmetric, and deep rift basins (Model RM2, Fig. 5.3), whereas decoupled scenarios lead to an asymmetric, and shallower rift (Models RM3, RM3b, FM1; Figs. 5.4, 5.5, 5.6).

The sediment pile in shallow basins is usually not enough to provide conditions for hydrocarbon generation, due to its low temperature and pressure. So, in this case, the compositional inheritance that affected the coupling between the crust and the mantle might have directly affected the economic potential of the Cariri Valley basins.

Furthermore, in cases where hydrocarbon generation and migration happened, structural inheritances usually serve as pathways to oil and gas migration during rift- and post-rift phases (BOSWORTH & TARI, 2021; RAMOS *et al.*, 2022). Also, according to TAO *et al.* (2022), structural inheritances are strongly related to overpressure in sedimentary basins. Fluids circulation along faults may lead to hydrothermal silicification, transforming the faults into impermeable barriers (RAMOS *et al.*, 2022; SIBSON, 1990; TAO *et al.*, 2022). Confined fluids deep below the surface create the perfect environment for overpressure. During drilling operations, overpressured zones usually represent an operational risk because it may lead to kicks and blowouts. Therefore, recognizing these zones is a matter of great importance (TAO *et al.*, 2022, and references therein).

Chapter 7

Conclusions

The Proterozoic inheritance is a matter of great importance when studying the formation of the continental rift basins in northeastern Brazil (Fig. 2.4), as seen in the works of MATOS (1999, 1992); MATOS *et al.* (2021); RAMOS *et al.* (2022).

Numerical models represented a novel approach to investigating the basin formation in northeastern Brazil because they allowed us to test different lithospheric settings and how they affect the rifting process.

The scenarios presented in this paper show that:

- The strong rheology of the shear zones delimited the rifting in the upper crust after it had already started, rather than localizing it since the onset of rifting. That is, the nucleation of faults described in MATOS (1999) (Fig. 2.4) occurred after the initial lithospheric necking, not before;

- Rifting location occurs in weak layers within the lithosphere, and mantelic heterogeneities have a major role in strain localization when compared to crustal heterogeneities (e.g., ALESSANDRO *et al.*, 2023; CHENIN & BEAUMONT, 2013; CHENIN *et al.*, 2019; MANATSCHAL *et al.*, 2015);

- The lateral heterogeneity of the lithospheric mantle is a main driver for rift nucleation. This means that the contact of portions with different degrees of rigidity creates boundary effects for the nucleation of plastic deformations.;

- Strong (upper) crustal inheritances (i.e., mylonitic shear zones) may control the deformation on a crustal scale only (MANATSCHAL *et al.*, 2015);

- Although being weak terranes, the Cachoeirinha Seridó and Cariris-Velhos belts were not rifted due to the higher degree of lithospheric coupling when compared to the "normal" Paleoproterozoic basement;

- During the rifting of the Borborema Province, elevated rift shoulders were formed on both sides of the Cariri Valley along with central areas of topo-

graphic low, which may extend to NE and SW. This scenario allowed marine incursion from the NE direction, through the newly formed Potiguar Basin, which agrees with provenance studies based on U-Pb dating of detrital zircons from sandstones of the Araripe Basin (SOUZA *et al.*, 2022);

- Coupling between the upper-crust and the lithospheric mantle affects the way strain is distributed across the lithosphere (BUROV *et al.*, 2006), impacting the distribution and geometry of rifts. It may be related to the economic potential of a sedimentary basin, as the depth is a relevant factor for hydrocarbon generation.

Bibliography

ALESSANDRO, D., ANDREA, C., ALBERTO, Z., et al., 2023, "The Ivrea-Verbano tectonic evolution: The role of the crust-mantle interactions in rifting localization", *Earth-Science Reviews*, p. 104318.

ALMEIDA, F. F. M., HASUI, Y., BRITO NEVES, B. B., et al., 1981, "Brazilian structural provinces: An introduction", *Earth-science reviews*, v. 17, n. 1-2, pp. 1–29.

ARAI, M., 2014, "Aptian/Albian (Early Cretaceous) paleogeography of the South Atlantic: a paleontological perspective", *Brazilian Journal of Geology*, v. 44, pp. 339–350.

ARAI, M., 2016, "Reply to the comments of Assine et al.(Comments on paper by M. Arai" Aptian/Albian (Early Cretaceous) paleogeography of the South Atlantic: a paleontological perspective")", *Brazilian Journal of Geology*, v. 46, pp. 09–13.

ARTHAUD, M. H., CABY, R., FUCK, R. A., et al., 2008, "Geology of the northern Borborema Province, NE Brazil and its correlation with Nigeria, NW Africa", *Geological Society of London, Special Publications*, v. 294, n. 1, pp. 49–67.

ASSINE, M. L., 1992, "Análise estratigráfica da bacia do Araripe, Nordeste do Brasil", *Brazilian Journal of Geology*, v. 22, n. 3, pp. 289–300.

ASSINE, M. L., 2007, "Bacia do Araripe", *Boletim de Geociências da PETRO-BRAS*, v. 15, n. 2, pp. 371–389.

ASSINE, M. L., PERINOTTO, J. D. J., CUSTÓDIO, M. A., et al., 2014, "Sequências deposicionais do andar Alagoas da Bacia do Araripe, nordeste do Brasil", *Boletim de Geociências da Petrobras*, v. 22, n. 1, pp. 3–28.

BALAY, S., GROPP, W. D., MCINNES, L. C., et al., 1997, "Efficient Management of Parallelism in Object Oriented Numerical Software Libraries". In: Arge,

E., Bruaset, A. M., Langtangen, H. P. (Eds.), *Modern Software Tools in Scientific Computing*, pp. 163–202. Birkhäuser Press.

BALAY, S., ABHYANKAR, S., ADAMS, M. F., et al., 2019. "PETSc Web page". `https://www.mcs.anl.gov/petsc`. Available at: <`https://www.mcs.anl.gov/petsc`>.

BALAY, S., ABHYANKAR, S., ADAMS, M. F., et al., 2020, *PETSc Users Manual*. Relatório Técnico ANL-95/11 - Revision 3.14, Argonne National Laboratory. Available at: <`https://www.mcs.anl.gov/petsc`>.

BONIFACIO, J. F., GANADE, C. E., DOS SANTOS, A. C., et al., 2023, "Review and critical assessment on plate reconstruction models for the South Atlantic", *Earth-Science Reviews*, p. 104333.

BOSWORTH, W., TARI, G., 2021, "Hydrocarbon accumulation in basins with multiple phases of extension and inversion: examples from the Western Desert (Egypt) and the western Black Sea", *Solid Earth*, v. 12, n. 1, pp. 59–77.

BRAUN, J., 2003, "Pecube: A new finite-element code to solve the 3D heat transport equation including the effects of a time-varying, finite amplitude surface topography", *Computers & Geosciences*, v. 29, n. 6, pp. 787–794.

BRITO NEVES, B. B., SANTOS, E. J., VAN SCHMUS, W. R., 2000, "The History of the Borborema Province, Northeastern Brazil". In: Cordani, U., Milani, E., Thomaz-Filho, A., et al. (Eds.), *Tectonic Evolution of South America*, v. 1, 31st International Geological Congress, pp. 151–182, Rio de Janeiro.

BRITO NEVES, B., FUCK, R. A., PIMENTEL, M. M., 2014, "The Brasiliano collage in South America: a review", *Brazilian Journal of Geology*, v. 44, pp. 493 – 518. doi: https://doi.org/10.5327/Z2317-4889201400030010.

BRUNE, S., HEINE, C., PÉREZ-GUSSINYÉ, M., et al., 2014, "Rift migration explains continental margin asymmetry and crustal hyper-extension", *Nature communications*, v. 5, n. 1, pp. 1–9.

BUROV, E. B., 2015, "Plate Rheology and Mechanics". In: Schubert, G. (Ed.), *Treatise on Geophysics: Crustal and Lithosphere Dynamics*, v. 6, 2 ed., Elsevier B.V., pp. 95–152, The Netherlands.

BUROV, E., WATTS, A., OTHERS, 2006, "The long-term strength of continental lithosphere:" jelly sandwich" or" crème brûlée"?" *GSA today*, v. 16, n. 1, pp. 4.

BYERLEE, J., 1978, "Friction of rocks", *Pure and Applied Geophysics*, v. 116, pp. 615–626. doi: https://doi.org/10.1007/BF00876528.

CABY, R., SIAL, A. N., ARTHAUD, M., et al., 1991, "Crustal Evolution and the Brasiliano Orogeny in Northeast Brazil". In: *The West African Orogens and Circum-Atlantic Correlatives*, IGCP-Project 233, Springer Berlin Heidelberg, pp. 373–397, Berlin, Heidelberg.

CHENIN, P., BEAUMONT, C., 2013, "Influence of offset weak zones on the development of rift basins: Activation and abandonment during continental extension and breakup", *Journal of Geophysical Research: Solid Earth*, v. 118, n. 4, pp. 1698–1720.

CHENIN, P., PICAZO, S., JAMMES, S., et al., 2019, "Potential role of lithospheric mantle composition in the Wilson cycle: a North Atlantic perspective", *Geological Society, London, Special Publications*, v. 470, n. 1, pp. 157–172.

CLOETINGH, S., ZIEGLER, P., BEEKMAN, F., et al., 2015, In: Schubert, G. (Ed.), *Tectonic Models for the Evolution of Sedimentary Basins*, v. 6, 2 ed., Elsevier B.V., pp. 513–553, The Netherlands.

CORTI, G., VAN WIJK, J., CLOETINGH, S., et al., 2007, "Tectonic inheritance and continental rift architecture: Numerical and analogue models of the East African Rift system", *Tectonics*, v. 26, n. 6.

DANTAS, E., SOUZA, Z., WERNICK, E., et al., 2013, "Crustal growth in the 3.4-2.7 Ga São José de Campestre Massif, Borborema Province, NE Brazil", *Precambrian Research*, v. 227, pp. 120 – 156. doi: https://doi.org/10.1016/j.precamres.2012.08.006.

FAMBRINI, G. L., SILVESTRE, D. D. C., BARRETO JUNIOR, A. M., et al., 2020, "Estratigrafia da Bacia do Araripe: estado da arte, revisão crítica e resultados novos", .

GANADE, C. E., WEINBERG, R. F., CORDANI, U. G., 2014, "Extruding the Borborema Province (NE-Brazil): a two-stage Neoproterozoic collision process", *Terra Nova*, v. 26, n. 2, pp. 157–168.

GANADE, C. E., WEINBERG, R. F., CAXITO, F. A., et al., 2021, "Decratonization by rifting enables orogenic reworking and transcurrent dispersal of old terranes in NE Brazil", *Scientific reports*, v. 11, n. 1, pp. 1–13.

GANADE, C. E., CIOFFI, C. R., MACHADO, J. P., et al., 2022, "Recurrent tectonic activity in northeastern Brazil during Pangea breakup: Constraints from U-Pb carbonate dating", *Geology*.

GERYA, T., 2010, *Introduction to Numerical Geodynamic Modelling*. 1 ed. New York, Cambridge University Press.

GERYA, T. V., YUEN, D. A., 2003, "Characteristics-based marker-in-cell method with conservative finite-differences schemes for modeling geological flows with strongly variable transport properties", *Physics of the Earth and Planetary Interiors*, v. 140, n. 4, pp. 293–318.

GLEASON, G. C., TULLIS, J., 1995, "A flow law for dislocation creep of quartz aggregates determined with the molten salt cell", *Tectonophysics*, v. 247, n. 1-4, pp. 1–23.

HEINE, C., ZOETHOUT, J., MÜLLER, R. D., 2013, "Kinematics of the South Atlantic rift", *Solid Earth*, v. 4, n. 2, pp. 215–253. doi: 10.5194/se-4-215-2013.

HOLLANDA, M. H. B. M., ARCHANJO, C. J., MACEDO FILHO, A. A., et al., 2018, "The Mesozoic Equatorial Atlantic Magmatic Province (EQUAMP): A New Large Igneous Province in South America". In: *Dyke Swarms of the World: A Modern Perspective*, Springer Singapore, pp. 87–110, Singapore.

HUGHES, T. J., 2012, *The finite element method: linear static and dynamic finite element analysis*. Courier Corporation.

HUISMANS, R. S., BEAUMONT, C., 2014, "Rifted continental margins: The case for depth-dependent extension", *Earth and Planetary Science Letters*, v. 407, pp. 148–162.

HUISMANS, R. S., BEAUMONT, C., 2003, "Symmetric and asymmetric lithospheric extension: Relative effects of frictional-plastic and viscous strain softening", *Journal of Geophysical Research: Solid Earth*, v. 108, n. B10.

KARATO, S.-I., WU, P., 1993, "Rheology of the upper mantle: A synthesis", *Science*, v. 260, n. 5109, pp. 771–778.

KROTH, M., BORGHI, L., BOBCO, F. E., et al., 2021, "Aptian shell beds from the Romualdo Formation (Araripe Basin): Implications for paleoenvironment and paleogeographical reconstruction of the Northeast of Brazil", *Sedimentary Geology*, v. 426, pp. 106025.

LOPES, L., GANADE, C., REIS, R., et al., 2019, "Cretaceous reactivation of the Neoproterozoic Pernambuco shear zone in NE-Brazil: initial results based on LA-ICP-MS U-Pb dating of calcite infilling in faults." 06. doi: 10.13140/RG.2.2.11367.91044.

LUZ, R., JULIÀ, J., DO NASCIMENTO, A., 2015, "Bulk crustal properties of the Borborema Province, NE Brazil, from P-wave receiver functions: Implications for models of intraplate Cenozoic uplift", *Tectonophysics*, v. 644, pp. 81–91.

MAISEY, J. G., 2000, "Continental break up and the distribution of fishes of Western Gondwana during the Early Cretaceous", *Cretaceous Research*, v. 21, n. 2-3, pp. 281–314.

MANATSCHAL, G., LAVIER, L., CHENIN, P., 2015, "The role of inheritance in structuring hyperextended rift systems: Some considerations based on observations and numerical modeling", *Gondwana Research*, v. 27, n. 1, pp. 140–164.

MANATSCHAL, G., CHENIN, P., LESCOUTRE, R., et al., 2021, "The role of inheritance in forming rifts and rifted margins and building collisional orogens: a Biscay-Pyrenean perspective", *BSGF-Earth Sciences Bulletin*, v. 192, n. 1, pp. 55.

MATOS, R. M. D., 2000, "Tectonic Evolution of the Equatorial South Atlantic". In: *Atlantic Rifts and Continental Margins*, American Geophysical Union, pp. 331–354, Washington, D. C.

MATOS, R. M. D., 1999, "History of the northeast Brazilian rift system: kinematic implications for the break-up between Brazil and West Africa", v. 153, n. 1, pp. 55–73.

MATOS, R. M. D., 1992, "The Northeast Brazilian Rift System", *Tectonics*, v. 11, n. 4, pp. 766–791.

MATOS, R. M. D., KRUEGER, A., NORTON, I., et al., 2021, "The fundamental role of the Borborema and Benin–Nigeria provinces of NE Brazil and NW Africa during the development of the South Atlantic Cretaceous Rift system", *Marine and petroleum geology*, v. 127, pp. 104872. doi: https://doi.org/10.1016/j.marpetgeo.2020.104872.

MILANI, E. J., DAVISON, I., 1988, "Basement control and transfer tectonics in the Recôncavo-Tucano-Jatobá rift, Northeast Brazil", *Tectonophysics*, v. 154, n. 1-2, pp. 41–70.

MIRANDA, T. S., NEVES, S. P., CELESTINO, M. A. L., et al., 2020, "Structural evolution of the Cruzeiro do Nordeste shear zone (NE Brazil): Brasiliano-Pan-African-ductile-to-brittle transition and Cretaceous brittle reactivation", *Journal of Structural Geology*, v. 141, pp. 104203.

MOHRIAK, W. U., BASSETTO, M., VIEIRA, I. S., 2000, "Tectonic Evolution of the Rift Basins in the Northeastern Brazilian Region". In: *Atlantic Rifts and Continental Margins*, American Geophysical Union, pp. 293–315, Washington, D. C.

MORAES, A., 2016, *Mecânica do Contínuo para a Geologia Estrutural*. 2 ed. São Paulo, Perse.

MORAIS NETO, J., HEGARTY, K., KARNER, G., 2006, "Abordagem preliminar sobre paleotemperatura e evolução do relevo da bacia do Araripe, Nordeste do Brasil, a partir da análise de traços de fissão em apatita", *Boletim de Geociências da Petrobras*, v. 14, n. 1, pp. 113–119.

MUÑOZ-BARRERA, J. M., ROTEVATN, A., GAWTHORPE, R. L., et al., 2020, "The role of structural inheritance in the development of high-displacement crustal faults in the necking domain of rifted margins: The Klakk Fault Complex, Frøya High, offshore mid-Norway", *Journal of Structural Geology*, v. 140, pp. 104163.

NEUMANN, V. H., BORREGO, A., CABRERA, L., et al., 2003, "Organic matter composition and distribution through the Aptian–Albian lacustrine sequences of the Araripe Basin, northeastern Brazil", *International Journal of Coal Geology*, v. 54, n. 1-2, pp. 21–40.

NEVES, S. P., 2003, "Proterozoic history of the Borborema province (NE Brazil): Correlations with neighboring cratons and Pan-African belts and implications for the evolution of western Gondwana", *Tectonics*, v. 22, n. 4, pp. 1031–n/a.

NOGUEIRA, F. C., MARQUES, F. O., BEZERRA, F. H., et al., 2015, "Cretaceous intracontinental rifting and post-rift inversion in NE Brazil: Insights from the Rio do Peixe Basin", *Tectonophysics*, v. 644, pp. 92–107.

NYBLADE, A. A., BRAZIER, R. A., 2002, "Precambrian lithospheric controls on the development of the East African rift system", *Geology*, v. 30, n. 8, pp. 755–758.

OLIVEIRA, R. G., MEDEIROS, W. E., 2018, "Deep crustal framework of the Borborema Province, NE Brazil, derived from gravity and magnetic data", *Precambrian research*, v. 315, pp. 45–65.

PESSANO, P. C., GANADE, C. E., TUPINAMBÁ, M., et al., 2021, "Updated map of the mafic dike swarms of Brazil based on airborne geophysical data", *Journal of South American Earth Sciences*, v. 107. doi: https://doi.org/10.1016/j.jsames.2020.103076.

RAMOS, G. V., VASCONCELOS, D. L., MARQUES, F. O., et al., 2022, "Relations between inherited basement fabric and fault nucleation in a continental setting: The Rio do Peixe Basin, NE Brazil", *Marine and Petroleum Geology*, v. 139, pp. 105635.

RICHETTI, P. C., ZWAAN, F., SCHREURS, G., et al., 2022, "Analogue modelling of basin inversion: the role of oblique kinematics and implications for the Araripe Basin (Brazil)", *EGUsphere*, pp. 1–33.

RING, U., 1994, "The influence of preexisting structure on the evolution of the Cenozoic Malawi rift (East African rift system)", *Tectonics*, v. 13, n. 2, pp. 313–326.

ROSA, M. C., MORALES, N., ASSINE, M. L., 2023, "Transtensional tectonics during the Gondwana breakup in northeastern Brazil: Early Cretaceous paleostress inversion in the Araripe Basin", *Tectonophysics*, v. 846, pp. 229666.

SACEK, V., 2017, "Post-rift influence of small-scale convection on the landscape evolution at divergent continental margins", *Earth and Planetary Science Letters*, v. 459, pp. 48–57.

SACEK, V., ASSUNÇÃO, J., PESCE, A., et al., 2022, "Mandyoc: A finite element code to simulate thermochemical convection in parallel", *Journal of Open Source Software*, v. 7, n. 71, pp. 4070. doi: 10.21105/joss.04070. Available at: <`https://doi.org/10.21105/joss.04070`>.

SALAZAR-MORA, C. A., SACEK, V., 2021, "Lateral flow of thick continental lithospheric mantle during tectonic quiescence", *Journal of Geodynamics*, v. 145, pp. 101830.

SALGADO-CAMPOS, V. M. J., DE SOUZA CARVALHO, I., BERTOLINO, L. C., et al., 2021, "Clay mineralogy and lithogeochemistry of lutites from the Lower Cretaceous Crato Member, Araripe Basin, NE Brazil: Implications

for paleoenvironmental, paleoclimatic and provenance reconstructions", *Journal of South American Earth Sciences*, v. 110, pp. 103329.

SAMSU, A., CRUDEN, A. R., MICKLETHWAITE, S., et al., 2020, "Scale matters: The influence of structural inheritance on fracture patterns", *Journal of Structural Geology*, v. 130, pp. 103896.

SCHIFFER, C., DORÉ, A. G., FOULGER, G. R., et al., 2020, "Structural inheritance in the North Atlantic", *Earth-Science Reviews*, v. 206, pp. 102975.

SIBSON, R. H., 1990, "Conditions for fault-valve behaviour", *Geological Society, London, Special Publications*, v. 54, n. 1, pp. 15–28.

SILVA, R. D., SACEK, V., 2022, "Influence of Surface Processes on Postrift Faulting During Divergent Margins Evolution", *Tectonics*, v. 41, n. 2, pp. e2021TC006808.

SOUZA, J. F. G., ISOZAKI, Y., TSUTSUMI, Y., et al., 2022, "Provenance analysis of the Araripe intracontinental basin, northeast Brazil–Routes for proto-Atlantic marine incursions in northwest Gondwana", *Sedimentary Geology*, v. 440, pp. 106243.

SPIGOLON, A. L., LEWAN, M. D., DE BARROS PENTEADO, H. L., et al., 2015, "Evaluation of the petroleum composition and quality with increasing thermal maturity as simulated by hydrous pyrolysis: A case study using a Brazilian source rock with Type I kerogen", *Organic Geochemistry*, v. 83, pp. 27–53.

STÜWE, K., 2007, *Geodynamics of the Lithosphere: An Introduction*. 2 ed. Berlin, Heidelberg, Springer Berlin / Heidelberg.

SZATMARI, P., FRANCOLIN, J., ZANOTTO, O., et al., 1987, "Evolução tectônica da margem equatorial brasileira", *Revista Brasileira de Geociências*, v. 17, pp. 180–188. doi: 10.25249/0375-7536.1987180188.

TACKLEY, P. J., KING, S. D., 2003, "Testing the tracer ratio method for modeling active compositional fields in mantle convection simulations", *Geochemistry, Geophysics, Geosystems*, v. 4, n. 4.

TAO, Z., HE, Z., ALVES, T. M., et al., 2022, "Structural inheritance and its control on overpressure preservation in mature sedimentary basins (Dongying depression, Bohai Bay Basin, China)", *Marine and Petroleum Geology*, v. 137, pp. 105504.

THIEULOT, C., 2014, "ELEFANT: a user-friendly multipurpose geodynamics code", *Solid Earth Discuss*, v. 6, pp. 1949–2096.

TOMMASI, A., VAUCHEZ, A., 2001, "Continental rifting parallel to ancient collisional belts: an effect of the mechanical anisotropy of the lithospheric mantle", *Earth and Planetary Science Letters*, v. 185, n. 1-2, pp. 199–210.

VAN SCHMUS, W., KOZUCH, M., DE BRITO NEVES, B. B., 2011, "Precambrian history of the Zona Transversal of the Borborema Province, NE Brazil: Insights from Sm–Nd and U–Pb geochronology", *Journal of South American Earth Sciences*, v. 31, n. 2-3, pp. 227–252.

VAUCHEZ, A., NEVES, S., CABY, R., et al., 1995, "The Borborema shear zone system, NE Brazil", *Journal of South American earth sciences*, v. 8, n. 3, pp. 247–266.

VIOLA, G., ANDREOLI, M., BEN-AVRAHAM, Z., et al., 2005, "Offshore mud volcanoes and onland faulting in southwestern Africa: neotectonic implications and constraints on the regional stress field", *Earth and Planetary Science Letters*, v. 231, n. 1, pp. 147–160.

VIOLA, G., KOUNOV, A., ANDREOLI, M. A. G., et al., 2012, "Brittle tectonic evolution along the western margin of South Africa: More than 500 Myr of continued reactivation", *Tectonophysics*, v. 514, pp. 93–114.

WILL, T. M., FRIMMEL, H. E., 2018, "Where does a continent prefer to break up? Some lessons from the South Atlantic margins", *Gondwana research*, v. 53, pp. 9–19.

ZHONG, S., YUEN, D. A., MORESI, L. N., et al., 2007, "Numerical methods for mantle convection", *Treatise on geophysics*, v. 7, pp. 227–252.